Mathematical Analysis of Low-Dimensional Reaction Network Systems

By

Yida Ding

A dissertation submitted in partial fulfillment

of the requirements for the degree of

Doctor of Philosophy

(Mathematics)

at the

UNIVERSITY OF WISCONSIN – MADISON

2020

Date of final oral examination: Dec 3, 2020

The dissertation is approved by the following members of the Final Oral Committee:

Gheorghe Craciun, Professor, Mathematics

David F. Anderson, Vilas Distinguished Achievement Professor , Mathematics

Laurentiu-George Maxim, Professor, Mathematics

Abhishek Deshpande, Visiting Assistant Professor, Mathematics

Abstract

Mathematical models of biochemical reaction networks and biological interaction networks are usually nonlinear, high dimensional, and have many unknown parameters. Moreover, these networks may be contained inside larger networks, and may be subject to external influences from the larger networks, which makes it even more challenging to analyze them mathematically. Here we address these challenges by looking at *variable-k dynamical systems*, either directly or by embedding them into *toric differential inclusions*.

Our main focus will be on *minimal invariant regions* and *minimal globally attracting regions* for both variable-k dynamical systems and toric differential inclusions. In the construction of the minimal invariant regions and globally attracting regions for toric differential inclusions, we will assume that the positive parameter δ (from the definition of toric differential inclusions) is large enough, in order to simplify their geometric properties. Moreover, transforming these dynamical systems from the original "exponential space" into the "logarithmic space" also gives a more explicit geometric understanding of these systems, especially in the large scale.

Toric differential inclusions occur as key dynamical systems for the study of large classes of mass-action systems, such as weakly reversible or endotactic systems, and in particular in the context of the Global Attractor Conjecture. We describe a procedure for explicitly constructing the minimal invariant and minimal globally attracting regions for two-dimensional toric differential inclusions. In particular, we obtain invariant regions and globally attracting regions for two-dimensional weakly reversible or endotactic dynamical systems (even if they have time-dependent parameters).

We obtain similar results for *variable-k dynamical systems*. The nature of invariant and globally attracting regions is fundamental to understanding the dynamical properties of non-autonomous reaction networks. We explicitly describe the construction of the minimal invariant regions and minimal globally attracting regions for dynamical systems consisting of two reversible reactions, where the rate constants are allowed to take values in a bounded interval.

Furthermore, we present some examples and results for *fixed-k* mass-action systems, which suggest interesting open problems.

Acknowledgements

First of all, I would like to extend my sincere gratitude to Professor Gheorghe Craciun. George has taught me how to come up with a question, how to read and study the background knowledge, how to think and discuss with a group of people, how to write and improve a paper. With his illuminating instruction, I learned that mathematics is not only about solving problems, it is also a systematic way of thinking and acting. I cannot thank him enough for his great patience during countless hours of discussions and his persistent encouragement during my graduate study.

Second, I would like to express my heartfelt gratitude to my collaborator Abhishek Deshpande for his persistent contribution to our projects. His critical thinking always leads us to some more comprehensive solutions in our projects. My sincere thanks also go to Professor David F. Anderson, for his great help and support.

I would like to thank Polly, Jiaxin and Jenny for their invaluable comments and suggestions in our group discussions.

Last but not the least, my greatest thanks go to my parents for their considerations and great confidence in me all through these years.

List of Figures

Contents

Chapter 1

Introduction

1.1 Introduction

A wide range of mathematical models in biology, chemistry, physics, and engineering are governed by interactions between various populations. Often these systems can be represented by a set of differential equations on the positive orthant with polynomial or power-law right-hand sides, i.e., they have the form

$$\frac{d\boldsymbol{x}}{dt} = \sum_{i=1}^{m} \boldsymbol{x}^{\boldsymbol{s}_i} \boldsymbol{v}_i \tag{1.1.1}$$

where $\boldsymbol{x} = (x_1, x_2, ..., x_n) \in \mathbb{R}^n_{>0}$, $\boldsymbol{s}_i, \boldsymbol{v}_i \in \mathbb{R}^n$, and $\boldsymbol{x}^{\boldsymbol{y}} := x_1^{y_1} x_2^{y_2} ... x_n^{y_n}$. Here, we are concerned with the more general class of dynamical systems of the form

$$\frac{d\boldsymbol{x}}{dt} = \sum_{i=1}^{m} k_i(t) \boldsymbol{x}^{\boldsymbol{s}_i} \boldsymbol{v}_i \tag{1.1.2}$$

where we allow the coefficients $k_i \in \mathbb{R}^+$ to vary in time, but we assume that there exist some $\epsilon > 0$ such that $\epsilon < k_i < \frac{1}{\epsilon}$ for all $t > 0$. We refer to such systems as *variable-k polynomial dynamical systems*. A key dynamical property of such systems is *persistence* which essentially means that no species can go extinct. In particular, a solution $\boldsymbol{x}(t)$ of (1.1.1) is said to be *persistent* if for any initial condition $\boldsymbol{x}(0) \in \mathbb{R}^n_{>0}$, we have $\liminf_{t\to\infty} x_i(t) > 0$

for $i = 1, 2, ..., n$. The *Persistence Conjecture* says that dynamical systems generated by weakly reversible reaction networks are persistent [9]. This conjecture is related to the *Global Attractor Conjecture* which says that there exists a unique globally attracting equilibrium for complex balanced dynamical systems (up to linear conservation laws) [8]. Many special cases of the Global Attractor Conjecture have been proved [1, 9, 13, 19]. Recently, a proof of the Global Attractor Conjecture in the fully general case was proposed [4]. A key tool in this proof is the embedding of weakly reversible dynamical systems into *toric differential inclusions*, which are piecewise constant differential inclusions possessing a rich geometric structure [4, 5, 6]. It is known that positive solutions of toric differential inclusions are contained in some specific invariant regions [4]. In this paper, we focus on two-dimensional toric differential inclusions. We give an explicit procedure for constructing the minimal invariant regions and minimal globally attracting regions for toric differential inclusions. In particular, we can interpret our results as follows: two-dimensional complex balanced systems are known to have *globally attracting points* located in the strictly positive quadrant; similarly, the corresponding toric differential inclusions have *globally attracting compact sets*, which are also subsets of the strictly positive quadrant, and can be characterized in detail.

This thesis is structured as follows: In chapter 1, we give a brief introduction to reaction networks and mass-action systems. In chapter 2, we introduce some very useful definitions and theorems; in section 2.1 we introduce reaction networks as Euclidean embedded graphs, and we define the notions of persistence and permanence for dynamical systems generated by reaction networks; in section 2.2 we describe *complex-balanced systems* and *detailed-balanced systems*, then we mention the *Horn-Jackson theorem* and *Deficiency zero theorem* which specify the properties of *complexed-balanced steady states* and derive a sufficient condition for the existence of complexed-balanced steady states; in section 2.3 we rigorously define a polyhedral cone, polyhedral fan and *toric differential inclusions*; we also define *minimal invariant regions* and *minimal globally attracting regions* for toric differential

inclusions; in section 2.4 we define *minimal invariant regions* and *minimal globally attracting regions* in variable-k dynamical systems. In chapter 3, we describe the behavior of toric differential inclusion and variable-k dynamical systems in the logarithmic space; in section 3.1 we give an example of reversible dynamical systems and variable-k dynamical systems in exponential space and logarithmic space; in section 3.2 we describe the toric differential inclusions in the logarithmic space and we also mention a rescale method which simplifies the geometry when we change the parameter ϵ or δ along with the scaling in the logarithmic space; in section 3.3 we analyse the shape of bounded line segments in large scale logarithmic space which gives an intuition of how to simplify the trajectories bounded with proper cone in large scale logarithmic space. In chapter 4, by bringing in the toric differential inclusions, we construct a region $\mathcal{M}_{\mathcal{F},\delta}$ for a given set of polyhedral fans; we prove that the region $\mathcal{M}_{\mathcal{F},\delta}$ is both the minimal invariant region and the minimal globally attracting region for the given mass-action system; then we summarize the results, discuss some special cases and future questions. In chapter 5, we construct the minimal invariant region and the minimal globally attracting region in the variable-k dynamical system and we give a proof and some examples for the two reaction cases.

Chapter 2

Background: definitions and theorems

2.1 Euclidean embedded graphs, persistence, permanence

A *reaction network* is a directed graph $\mathcal{G} = (V, E)$ called the Euclidean embedded graph [4, 5, 6], where $V \subset \mathbb{R}^n$ is the set of vertices and E is the set of edges corresponding to the reactions in the network. We will abbreviate the Euclidean embedded graph by an E-graph. Note that if $\boldsymbol{y}, \boldsymbol{y}' \in V$ are two distinct vertices of the E-graph $\mathcal{G}$, then $\boldsymbol{y} \to \boldsymbol{y}' \in E$ means that there is a directed edge from $\boldsymbol{y}$ to $\boldsymbol{y}'$. An E-graph $\mathcal{G} = (V, E)$ is called *reversible* if $\boldsymbol{y} \to \boldsymbol{y}' \in E$ implies $\boldsymbol{y}' \to \boldsymbol{y} \in E$. An E-graph $\mathcal{G} = (V, E)$ is called *weakly reversible* if every edge $\boldsymbol{y} \to \boldsymbol{y}' \in E$ is part of some directed cycle. An E-graph $\mathcal{G} = (V, E)$ is called *endotactic* if for every $\boldsymbol{v} \in \mathbb{R}^n$ with $\boldsymbol{v} \cdot (\boldsymbol{y}' - \boldsymbol{y}) > 0$ for some $\boldsymbol{y} \to \boldsymbol{y}' \in E$, there exists a $\tilde{\boldsymbol{y}} \to \tilde{\boldsymbol{y}}' \in E$ such that $\boldsymbol{v} \cdot (\tilde{\boldsymbol{y}}' - \tilde{\boldsymbol{y}}) < 0$ and $\boldsymbol{v} \cdot \tilde{\boldsymbol{y}} > \boldsymbol{v} \cdot \boldsymbol{y}$. Given $\boldsymbol{x}^* \in \mathbb{R}^n_{>0}$, the *stoichiometric compatibility class* of $\boldsymbol{x}^*$ is the polyhedron $(\boldsymbol{x}^* + S) \cap \mathbb{R}^n_{>0}$, where $S = \text{span}\{\boldsymbol{y}' - \boldsymbol{y} \mid \boldsymbol{y} \to \boldsymbol{y}' \in E\}$.

Any E-graph $\mathcal{G} = (V, E)$ gives rise to a family of dynamical systems on the positive orthant. Under the standard assumption of mass-action kinetics [11, 14, 15, 23, 24] the dynamical systems generated by $\mathcal{G}$ can be represented as

$$\frac{d\boldsymbol{x}}{dt} = \sum_{\boldsymbol{y} \to \boldsymbol{y}' \in E} k_{\boldsymbol{y} \to \boldsymbol{y}'} \boldsymbol{x}^{\boldsymbol{y}} (\boldsymbol{y}' - \boldsymbol{y}) \tag{2.1.1}$$

where the parameter $k_{\boldsymbol{y}\to\boldsymbol{y}'} > 0$ is the *rate constant* corresponding to the reaction $\boldsymbol{y} \to \boldsymbol{y}'$. In general, rate constants can actually vary with time due to external signals or forcing, and this gives rise to more general *non-autonomous* dynamical systems of the form

$$\frac{d\boldsymbol{x}}{dt} = \sum_{\boldsymbol{y}\to\boldsymbol{y}'\in E} k_{\boldsymbol{y}\to\boldsymbol{y}'}(t)\boldsymbol{x}^{\boldsymbol{y}}(\boldsymbol{y}' - \boldsymbol{y}) \tag{2.1.2}$$

If there exists an $\epsilon > 0$ such that $\epsilon \leq k_{\boldsymbol{y}\to\boldsymbol{y}'}(t) \leq \frac{1}{\epsilon}$ for every $\boldsymbol{y} \to \boldsymbol{y}' \in E$, then we call such a dynamical system a *variable-k polynomial (or power-law) dynamical system* [5, 6, 9].

Some of the most relevant properties of these types of systems are expressed by the notions of *persistence* and *permanence* [21, 22]. A dynamical system of the form (2.1.2) is said to be *persistent* if for any initial condition $\boldsymbol{x}_0 \in \mathbb{R}^n_{>0}$, the solution $\boldsymbol{x}(t)$ satisfies

$$\liminf_{t\to T} \boldsymbol{x}_i(t) > 0 \tag{2.1.3}$$

for every $i = 1, 2, ..., n$, where T is the maximum time for which $\boldsymbol{x}(t)$ is well-defined. A dynamical system of the form (2.1.2) is said to be *permanent* if for every stoichiometric compatibility class $\mathcal{D}$ there exists a compact set $\mathcal{K} \subset \mathcal{D}$ such that, if $\boldsymbol{x}(0) \in \mathcal{D}$, then we have $\boldsymbol{x}(t) \in \mathcal{K}$ for all sufficiently large t. A dynamical system given by the form (2.1.1) is said to be *complex balanced* if there exists $\tilde{\boldsymbol{x}} \in \mathbb{R}^n_{>0}$ such that the following is true for every vertex $\boldsymbol{y} \in V$:

$$\sum_{\boldsymbol{y}\to\boldsymbol{y}'\in E} k_{\boldsymbol{y}\to\boldsymbol{y}'}\tilde{\boldsymbol{x}}^{\boldsymbol{y}} = \sum_{\boldsymbol{y}'\to\boldsymbol{y}\in E} k_{\boldsymbol{y}'\to\boldsymbol{y}}\tilde{\boldsymbol{x}}^{\boldsymbol{y}'}. \tag{2.1.4}$$

These notions are related to the following open conjectures.

i. **Persistence conjecture:** Dynamical systems generated by weakly reversible reaction networks are persistent.

ii. **Extended Persistence conjecture:** Variable-k dynamical systems generated by endotactic networks are persistent.

ii. **Permanence conjecture:** Dynamical systems generated by weakly reversible reaction networks are permanent.

iv. **Extended Permanence conjecture:** Variable-k dynamical systems generated by endotactic networks are permanent.

A proof of any one of the conjectures above would also imply the *Global Attractor Conjecture*, which says that complex balanced dynamical systems have a globally attracting point within any stoichiometric compatibility class. In recent years, there have been several attempts towards the resolution of these conjectures. Craciun, Nazarov and Pantea [9] have proved that two-dimensional variable-k endotactic dynamical systems are permanent. Pantea has extended this result to show that weakly reversible variable-k dynamical systems with two-dimensional stoichiometric subspace are permanent [19]. Anderson has proved the global attractor conjecture for complex balanced dynamical systems consisting of a *single linkage class* [1]. Gopalkrishnan, Miller and Shiu [13] have extended this result to show that *strongly endotactic* variable-k dynamical systems are permanent. Craciun has proposed a proof of the global attractor conjecture in full generality, using a method based on toric differential inclusions [4]. In particular, the proof uses the fact that solutions of toric differential inclusions are confined to certain invariant regions. Therefore, it is important to understand more about invariant regions of toric differential inclusions. In chapter 4, we give explicit constructions for minimal invariant regions and minimal globally attracting regions of toric differential inclusions in two dimensions and in chapter 5, we study the similar problem with variable-k dynamical systems.

2.2 Some important theorems

A state $\boldsymbol{x}_0$ of a mass-action system is a **complex-balanced steady state** if in the corresponding Eculidean embedded graph $\mathcal{G}$ at each vertex, the net input into each complex balances the net flow out of the complex at the state $\boldsymbol{x}_0$.

$$\sum_{\boldsymbol{y}\to\boldsymbol{y}'\in\mathcal{G}} k_{\boldsymbol{y}\to\boldsymbol{y}'}\boldsymbol{x}_0^{\boldsymbol{y}} = \sum_{\boldsymbol{y}'\to\boldsymbol{y}\in\mathcal{G}} k_{\boldsymbol{y}'\to\boldsymbol{y}}\boldsymbol{x}_0^{\boldsymbol{y}'} \tag{2.2.1}$$

In particular, if a system is not weakly reversible, then it cannot be a complex-balanced system.

In thermodynamics, a closed system can exchange energy (as heat or work) but not matter, which means every individual reaction should achieve a balance state itself in the system. In 1972, Horn and Jackson [17] defined the class of "complex-balanced systems" which obey the laws of closed systems in thermodynamics as a generalization of detailed-balanced systems.

Definition 2.2.1. A state $\boldsymbol{x}_0$ of a mass-action system is a **detailed-balanced steady state** if the network is reversible, and for every pair of reactions $\boldsymbol{y} \rightleftharpoons \boldsymbol{y}'$ forward flow and backward flow are balanced at $\boldsymbol{x}_0$.

$$k_{\boldsymbol{y}\to\boldsymbol{y}'}\boldsymbol{x}_0^{\boldsymbol{y}} = k_{\boldsymbol{y}'\to\boldsymbol{y}}\boldsymbol{x}_0^{\boldsymbol{y}'} \tag{2.2.2}$$

Definition 2.2.2. A **detailed-balanced system** is a mass-action system $(\mathcal{G}, \boldsymbol{k})$ that has at least one detailed-balanced steady state. A **complex-balanced system** is a mass-action system $(\mathcal{G}, \boldsymbol{k})$ that has at least one complex-balanced steady state.

Theorem 2.2.3 (**Horn-Jackson theorem**). *[17, 24] Consider a reaction network $\mathcal{G}$ and a constant reaction rate vector $\boldsymbol{k}$. Assume that the mass-action system generated by $(\mathcal{G}, \boldsymbol{k})$ has a complex-balanced steady state $\boldsymbol{x}^*$; in other words, $(\mathcal{G}, \boldsymbol{k})$ is a complex-balanced system. Then all the following properties hold:*

1. *All positive steady states are complex-balanced, and there is exactly one steady state within every stoichiometric compatibility class.*

2. *The set of complex-balanced steady states $\mathcal{Z}_k$ satisfies the equation $\ln \mathcal{Z}_k = \ln \boldsymbol{x}^* + S^{\perp}$ where S is the stoichiometric subspace of $\mathcal{G}$.*

3. *The function*
$$L(\boldsymbol{x}) = \sum_{j=1}^{n} x_i(\ln x_i - \ln x_i^* - 1) \tag{2.2.3}$$
is a strictly convex Lyapunov function of this system, defined on $\mathbb{R}^n_{>0}$ and with global minimum at $\boldsymbol{x} = \boldsymbol{x}^*$.

4. *Every positive steady state is locally asymptotically stable within its stoichiometric compatibility class.*

In practice, the existence of a complex-balanced steady state is difficult to check. According to Feinberg and Horn, [10,12,16] deficiency is a necessary condition to determine if a network is complex-balanced.

Definition 2.2.4. In a mass-action system generated by the Eculidean embedded graph $\mathcal{G}$, the **deficiency** of the network is $\delta = m - l - s$, while m is the number of nodes in the graph $\mathcal{G}$, and l is the number of connected components in the graph, s is the dimension of the stoichiometric subspace of the graph.

Theorem 2.2.5 (**Deficiency zero theorem**). *[10,12,16] .A mass-action system is complex-balanced for all values of its reaction rate constants if and only if it is weakly reversible and has deficiency zero.*

Example 2.2.6.

$$\begin{aligned} Y &\underset{k_2}{\overset{k_1}{\rightleftharpoons}} 2X \\ 2X &\underset{k_4}{\overset{k_3}{\rightleftharpoons}} X + 2Y \\ X + 2Y &\underset{k_6}{\overset{k_5}{\rightleftharpoons}} Y \end{aligned} \tag{2.2.4}$$

This network is reversible and has deficiency $\delta = 3 - 1 - 2 = 0$. Therefore, according to the deficiency zero theorem2.2.5, for all choice of rate constant $k_i \in (0, \infty)$, the network is complex-balanced. Furthermore, the Horn-Jackson theorem 2.2.3 applies, the mass-action system has a unique steady state within each stoichiometric compatibility class.

2.3 Polyhedral cones, fans and toric differential inclusions

Recall that a *polyhedral cone* [2] $C \subset \mathbb{R}^n$ is a set whose elements can be represented as a nonnegative linear combination of a finite set of vectors as follows

$$C = \left\{ \sum_{i=1}^{k} a_i \boldsymbol{v}_i | a_i \geq 0, \boldsymbol{v}_i \in \mathbb{R}^n \right\} \tag{2.3.1}$$

An *affine cone* is a set of the form $\boldsymbol{x}_0 + C$, where $\boldsymbol{x}_0 \in \mathbb{R}^n$ and C is a cone. In what follows, we might refer to affine cones simply as cones. The meaning will be clear from the

context.

The polar of a cone C will be denoted by C^o and is defined as follows:

$$C^o = \{\boldsymbol{w} \in \mathbb{R}^n \mid \boldsymbol{w} \cdot \boldsymbol{x} \leq 0 \, \textbf{for} \, \boldsymbol{x} \in C\} \tag{2.3.2}$$

Figure 2.1 gives a few examples illustrating the polar of a cone.

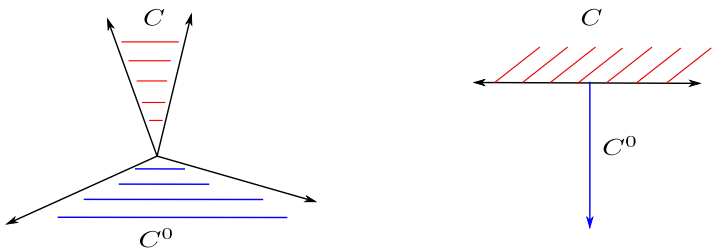

(a) (b)

Figure 2.1: A few examples showing the polar of a cone C. The cone C is marked in red and its polar C^o is marked in blue.

A *supporting hyperplane* H of a cone C is a hyperplane such that $H \cap C \neq \emptyset$ and C lies in exactly one of the half-spaces generated by H. A *face* of a cone is obtained by intersecting the cone with a supporting hyperplane. We now define the notion of a *polyhedral fan*.

Definition 2.3.1 (Polyhedral Fan)**.** A finite set $\mathcal{F}$ of polyhedral cones in $\mathbb{R}^n$ is a polyhedral fan if the following two conditions are satisfied:

(i) every face of a cone in $\mathcal{F}$ is also a cone in $\mathcal{F}$.

(ii) the intersection of any two cones in $\mathcal{F}$ is a face of both the cones.

If $\bigcup_{C \in \mathcal{F}} C = \mathbb{R}^n$, then the polyhedral fan $\mathcal{F}$ is said to be *complete*. Below, we define differential inclusions on the positive orthant. Differential inclusions differ from differential equations in the sense that the right hand side of a differential inclusion is allowed to take

values in a set instead of a single point as in the case of differential equations. They are vital to proving the persistence/permanence properties of various dynamical systems.

Definition 2.3.2 (Differential Inclusion)**.** A differential inclusion on $\mathbb{R}^n_{>0}$ is a dynamical system of the form

$$\frac{d\boldsymbol{x}}{dt} \in F(\boldsymbol{x}) \tag{2.3.3}$$

, where $F(\boldsymbol{x}) \subseteq \mathbb{R}^n$ for all $\boldsymbol{x} \in \mathbb{R}^n_{>0}$.

We now define toric differential inclusions, which are the key dynamical systems of interest in this thesis.

Definition 2.3.3 (Toric Differential Inclusions)**.** Given a complete polyhedral fan $\mathcal{F}$ and $\delta > 0$, a toric differential inclusion $\mathcal{T}_{\mathcal{F},\delta}$ is a dynamical system of the form

$$\frac{d\boldsymbol{x}}{dt} \in F_{\mathcal{F},\delta}(\boldsymbol{X}) \tag{2.3.4}$$

where $\boldsymbol{X} = \log \boldsymbol{x} \in \mathbb{R}^n$ and

$$F_{\mathcal{F},\delta}(\boldsymbol{X}) = \left(\bigcap_{\substack{C \in \mathcal{F} \\ dist(\boldsymbol{X}, C) \leq \delta}} C \right)^o . \tag{2.3.5}$$

From [7, Equation 9], Equation (2.3.5) can be written as

$$F_{\mathcal{F},\delta}(\boldsymbol{X}) = \left(\bigcap_{\substack{C\in\mathcal{F} \\ dist(\boldsymbol{X},C)\leq\delta \\ dim(C)=n}} C \right)^{o}. \tag{2.3.6}$$

Figure 2.2 depicts the toric differential inclusion for a fan consisting of two line generators.

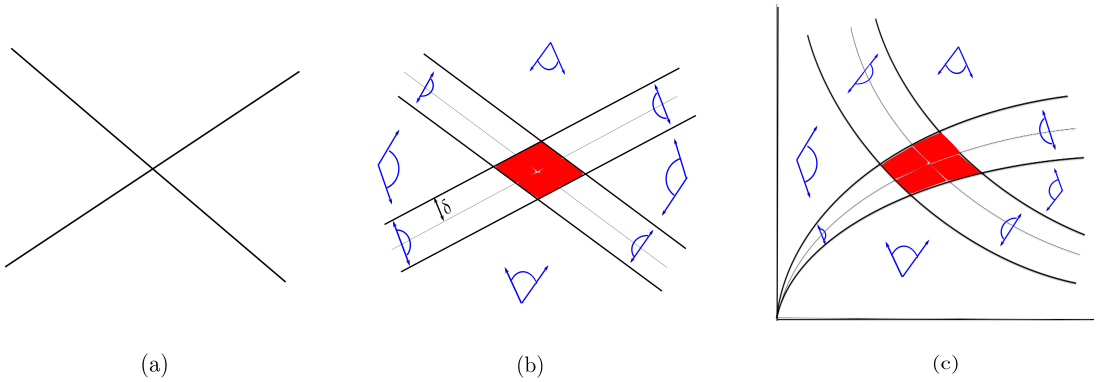

Figure 2.2: (a) Fan consisting of nine cones: four cones of dimension two, four cones of dimension one and one cone of dimension zero. (b) Lines parallel to and at a distance δ from the line generators in (a). The blue cones indicate the right hand side of the toric differential inclusion for regions of space far from the origin. The red part indicates the region of space where the right hand side of the toric differential inclusion is $\mathbb{R}^2$. (c) The curves obtained by exponentiating the lines in (b). The blue cones are unchanged from (b).

Definition 2.3.4 (Embedding)**.** A dynamical system of the form $\frac{d\boldsymbol{x}}{dt} = \boldsymbol{f}(\boldsymbol{x}, t)$ is said to be **embedded** into the differential inclusion $\frac{d\boldsymbol{x}}{dt} \in \boldsymbol{F}(\boldsymbol{x})$ if $\boldsymbol{f}(\boldsymbol{x}, t) \in \boldsymbol{F}(\boldsymbol{x})$ for every $\boldsymbol{x} \in \mathbb{R}^n_{>0}$ and all $t > 0$.

Definition 2.3.5 (Minimal invariant region)**.** Consider a toric differential inclusion $\mathcal{T}_{\mathcal{F},\delta}$. A

set $\Omega^{\mathbf{inv}}_{\mathcal{T}_{\mathcal{F},\delta}} \subseteq \mathbb{R}^n_{>0}$ is an **i**nvariant region of $\mathcal{T}_{\mathcal{F},\delta}$ if for any solution $\boldsymbol{x}(t)$ of $\mathcal{T}_{\mathcal{F},\delta}$ with $\boldsymbol{x}(0) \in \Omega^{\mathbf{inv}}_{\mathcal{T}_{\mathcal{F},\delta}}$, we have $\boldsymbol{x}(t) \in \Omega^{\mathbf{inv}}_{\mathcal{T}_{\mathcal{F},\delta}}$ for all $t > 0$. A set $\Omega^{\mathbf{min,inv}}_{\mathcal{T}_{\mathcal{F},\delta}}$ is the **m**inimal invariant region of $\mathcal{T}_{\mathcal{F},\delta}$ if for any invariant region $\Omega^{\mathbf{inv}}_{\mathcal{T}_{\mathcal{F},\delta}}$, we have $\Omega^{\mathbf{min,inv}}_{\mathcal{T}_{\mathcal{F},\delta}} \subseteq \Omega^{\mathbf{inv}}_{\mathcal{T}_{\mathcal{F},\delta}}$.

Definition 2.3.6. Consider a solution $\boldsymbol{x}(t)$ of the toric differential inclusion $\mathcal{T}_{\mathcal{F},\delta}$. We call $\boldsymbol{x}(t)$ a **strict solution** of $\mathcal{T}_{\mathcal{F},\delta}$ if for every compact set $K \subset \mathbb{R}^n_{>0}$, there exists $\rho > 0$ such that if $\boldsymbol{x}(t) \in K$ and $F_{\mathcal{F},\delta}(\log(\boldsymbol{x}(t)) \neq \mathbb{R}^n$, then $\|\frac{d\boldsymbol{x}(t)}{dt}\| > \rho$.

Definition 2.3.7 (Omega-limit set)**.** Consider a toric differential inclusion $\mathcal{T}_{\mathcal{F},\delta}$. Let $\boldsymbol{x}(t)$ be a solution of $\mathcal{T}_{\mathcal{F},\delta}$ with $\boldsymbol{x}(0) \in \mathbb{R}^n_{>0}$. Then, the **omega-limit set** of $\boldsymbol{x}(t)$ with initial condition $\boldsymbol{x}(0)$ is the set $\omega(\boldsymbol{x}(0)) = \{\boldsymbol{x}^* \in \mathbb{R}^n_{\geq 0}$: there exists a sequence of times $t_1 < t_2 < ... < t_k$ with $\lim_{k\to\infty} t_k = \infty$ such that $\lim_{k\to\infty} \boldsymbol{x}(t_k) = \boldsymbol{x}^*\}$.

Definition 2.3.8 (Minimal globally attracting region)**.** Consider a toric differential inclusion $\mathcal{T}_{\mathcal{F},\delta}$. A set $\Omega^{\mathbf{glob}}_{\mathcal{T}_{\mathcal{F},\delta}} \subseteq \mathbb{R}^n_{>0}$ is a **g**lobally attracting region of $\mathcal{T}_{\mathcal{F},\delta}$ if for any strict solution $\boldsymbol{x}(t)$ of $\mathcal{T}_{\mathcal{F},\delta}$ with $\boldsymbol{x}(0) \in \mathbb{R}^n_{>0}$, we have $\omega(\boldsymbol{x}(0)) \subseteq \Omega^{\mathbf{glob}}_{\mathcal{T}_{\mathcal{F},\delta}}$. A set $\Omega^{\mathbf{min,glob}}_{\mathcal{T}_{\mathcal{F},\delta}}$ is the **m**inimal globally attracting region of $\mathcal{T}_{\mathcal{F},\delta}$ if for any globally attracting region $\Omega^{\mathbf{glob}}_{\mathcal{T}_{\mathcal{F},\delta}}$, we have $\Omega^{\mathbf{min,glob}}_{\mathcal{T}_{\mathcal{F},\delta}} \subseteq \Omega^{\mathbf{glob}}_{\mathcal{T}_{\mathcal{F},\delta}}$.

Definition 2.3.9 (Trajectory)**.** Consider a toric differential inclusion $\mathcal{T}_{\mathcal{F},\delta}$ and points $P_1, P_2 \in \mathbb{R}^n_{>0}$. We will say that there is a **trajectory of** $\mathcal{T}_{\mathcal{F},\delta}$ from P_1 to P_2 if there exists a solution $\boldsymbol{x}(t)$ of $\mathcal{T}_{\mathcal{F},\delta}$ with $\boldsymbol{x}(0) = P_1$ such that for every $\zeta > 0$ there exists $t_0 > 0$ satisfying $||\boldsymbol{x}(t_0) - P_2|| < \zeta$.

2.4 Omega-limit set, invariant region and globally attracting region in variable-k dynamical systems

Similarly the invariant region and globally attracting region can be defined in variable-k dynamical systems, since the system may take infinite amount of time to reach the equilibrium state, we would use limit in our results.

Definition 2.4.1. Consider a dynamical system $\mathcal{G}_\epsilon^{\text{variable-k}}$. Let $\boldsymbol{x}(t)$ be a solution of $\mathcal{G}_\epsilon^{\text{variable-k}}$ with initial condition $\boldsymbol{x}(0) \in \mathbb{R}^n_{>0}$. The *omega-limit* of this solution is the set $\omega(\boldsymbol{x}(0)) = \{\boldsymbol{z} \in \mathbb{R}^n_{\geq 0} : \text{there is an increasing sequence of times } (t_h)_{h\in\mathbb{N}} \text{ such that } \lim_{h\to\infty} t_h = \infty \text{ and } \lim_{h\to\infty} \boldsymbol{x}(t_h) = \boldsymbol{z}\}$.

Definition 2.4.2. Consider a dynamical system $\mathcal{G}_\epsilon^{\text{variable-k}}$. A set $\Omega^{\text{inv}}_{\text{variable-k}} \in \mathbb{R}^n_{>0}$ is said to be an *invariant region* for $\mathcal{G}_\epsilon^{\text{variable-k}}$ if for any solution $\boldsymbol{x}(t)$ of $\mathcal{G}_\epsilon^{\text{variable-k}}$ with $\boldsymbol{x}(0) \in \Omega^{\text{inv}}_{\text{variable-k}}$, we have $\boldsymbol{x}(t) \in \Omega^{\text{inv}}_{\text{variable-k}}$ for all $t > 0$. A set $\Omega^{\text{min,inv}}_{\text{variable-k}}$ is said to be the *minimal invariant region* if for any invariant region $\Omega_{\text{variable-k}}$, we have $\Omega^{\text{min,inv}}_{\text{variable-k}} \subseteq \Omega_{\text{variable-k}}$.

Definition 2.4.3. Consider a dynamical system $\mathcal{G}_\epsilon^{\text{variable-k}}$. A set $\Omega^{\text{glob}}_{\text{variable-k}} \in \mathbb{R}^n_{>0}$ is said to be a *globally attracting region* for $\mathcal{G}_\epsilon^{\text{variable-k}}$ if for any solution $\boldsymbol{x}(t)$ of $\mathcal{G}_\epsilon^{\text{variable-k}}$ with $\boldsymbol{x}(0) \in \mathbb{R}^n_{>0}$, we have $\omega(\boldsymbol{x}(0)) \subseteq \Omega^{\text{glob}}_{\text{variable-k}}$. A set $\Omega^{\text{min,glob}}_{\text{variable-k}}$ is said to be the *minimal globally attracting region* if for any globally attracting region $\Omega_{\text{variable-k}}$, we have $\Omega^{\text{min,glob}}_{\text{variable-k}} \subseteq \Omega^{\text{glob}}_{\text{variable-k}}$.

Definition 2.4.4. Consider a dynamical system $\mathcal{G}_\epsilon^{\text{variable-k}}$. Given two points $P, Q \in \mathbb{R}^n_{>0}$, we say $P \rightsquigarrow_{\text{variable-k}} Q$ if there is a solution $\boldsymbol{x}(t)$ of $\mathcal{G}_\epsilon^{\text{variable-k}}$ such that $\boldsymbol{x}(0) = P$ and for every $\xi > 0$ there exists a T that satisfies $||x(T) - Q|| \leq \xi$.

Chapter 3

Logarithmic space and exponential space

3.1 Exponential space and logarithmic space

In mass-action systems, the solution will always stay in the positive orthant, and many of them have the governing differential equation with the polynomial or power-law right-hand side.

$$\frac{d\boldsymbol{x}}{dt} = \sum_{i=1}^{m} \boldsymbol{x}^{\boldsymbol{s}_i} \boldsymbol{v}_i \tag{3.1.1}$$

where $\boldsymbol{x} = (x_1, x_2, ..., x_n) \in \mathbb{R}^n_{>0}$, $\boldsymbol{s}_i, \boldsymbol{v}_i \in \mathbb{R}^n$, and $\boldsymbol{x}^{\boldsymbol{y}} := \boldsymbol{x}_1^{y_1} \boldsymbol{x}_2^{y_2} ... \boldsymbol{x}_n^{y_n}$.

Set $\boldsymbol{X} = \ln \boldsymbol{x}$, then $\boldsymbol{X} = (\ln x_1, \ln x_2, ..., \ln x_n) = (X_1, X_2, ..., X_n) \in \mathbb{R}^n$. By taking logarithm, we transform the system into the logarithmic space, and we would refer the original system as in the exponential space.

Usually, we are transforming the graph of polynomial dynamical systems or power-law dynamical systems from the exponential space to logarithmic space to simplify the geometry of the graph.

Example 3.1.1. Consider the system of reversible reactions

$$\begin{aligned} Y &\underset{k_2}{\overset{k_1}{\rightleftharpoons}} 2X \\ 2Y &\underset{k_4}{\overset{k_3}{\rightleftharpoons}} 2Y + X \\ X + 2Y &\underset{k_6}{\overset{k_5}{\rightleftharpoons}} Y \end{aligned} \tag{3.1.2}$$

Then the differential equation,

$$\begin{aligned} \frac{dx}{dt} &= 2k_1 y - 2k_2 x^2 + k_3 y^2 - k_4 x y^2 - k_5 x y^2 + k_6 y \\ \frac{dy}{dt} &= -k_1 y + k_2 x^2 - k_5 x y^2 + k_6 y \end{aligned} \tag{3.1.3}$$

If we set all the rate constant $k_i = 1$, then the equilibrium for each reaction can be found by solving the polynomial equations. For example, in the system above

$$Y \underset{k_2}{\overset{k_1}{\rightleftharpoons}} 2X \tag{3.1.4}$$

the first reversible reaction will reach the equilibrium if $y = \frac{k_2}{k_1} x^2$, i.e. the forward and backward reactions have the same rate. Given that $k_1 = k_2 = 1$, the equilibrium will be the curve $y = x^2$. Similarly, let $k_3 = k_4 = k_5 = k_6 = 1$, the other two equilibrium curves in the exponential space are $xy = 1$ and $y = 1$. The curves become straight lines in the logarithmic space. As shown in below,

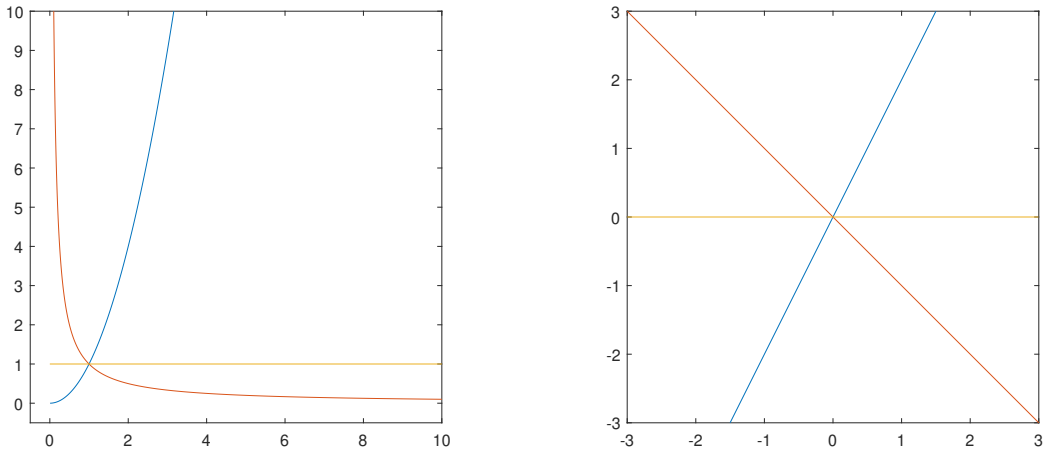

(a) The equilibrium of three reactions in exponential space with rate constant 1.

(b) The equilibrium of three reactions in logarithmic space with rate constant 1.

Figure 3.1

In variable-k dynamical systems, the rate constant $k_i \in [\epsilon, \frac{1}{\epsilon}]$, with $\epsilon \in (0, 1)$. Then the curves and lines become some regions. Every point in the region corresponds to a certain choose of $k_i \in [\epsilon, \frac{1}{\epsilon}]$. If we allow the coefficient $k_i(t)$ be functions of time vary in the closed interval $[\epsilon, \frac{1}{\epsilon}]$ then it leads to a non-autonomous dynamical system, which increases the uncertainties of the invariant sets and globally attracting sets in the system. We will discuss more about the variable-k dynamical systems in Chapter 5.

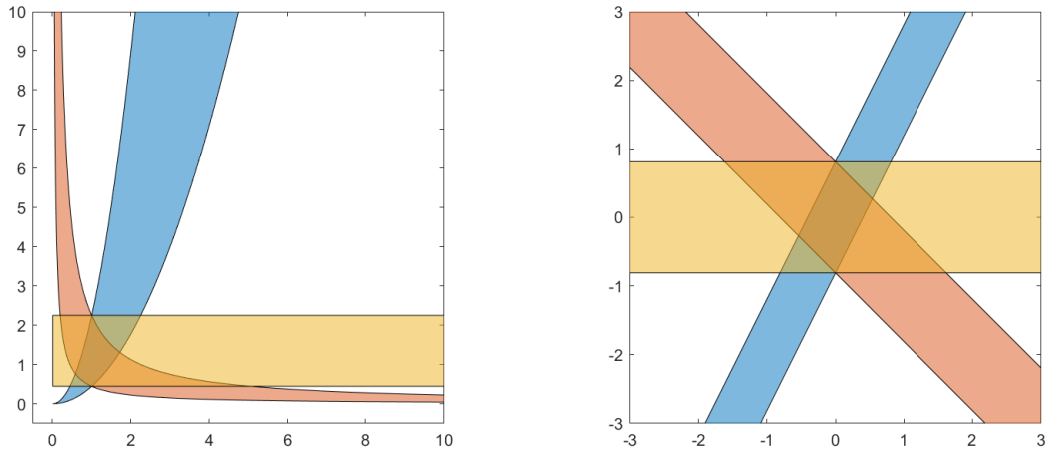

(a) The equilibrium regions of three reactions in exponential space in a variable-k dynamical system.

(b) The equilibrium regions of three reactions in logarithmic space in a variable-k dynamical system.

Figure 3.2

In this example, the curves of polynomial equations become lines in the logarithmic space. In the next section, we will show that how to use logarithmic space to solve a problem in large scale.

3.2 Toric differential inclusions in the logarithmic space

In the toric differential inclusions, we would start from a bunch of line generators, with some $\delta > 0$, there are some line regions with width 2δ in the logarithmic space, and then we can draw the corresponding curve regions in the exponential space.

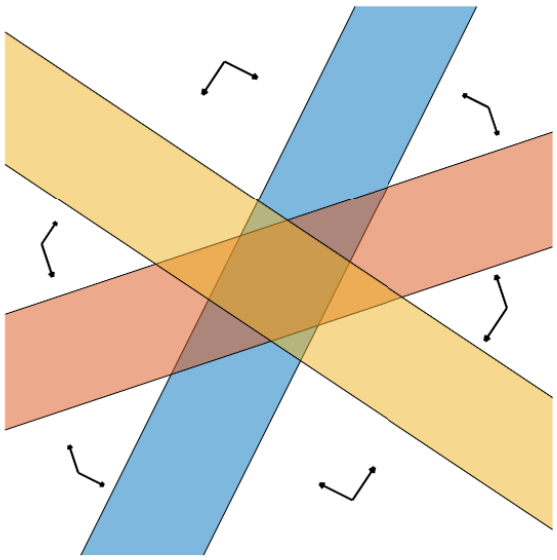

Figure 3.3: The line regions in logarithmic space(toric differential inclusions).

Figure 3.4

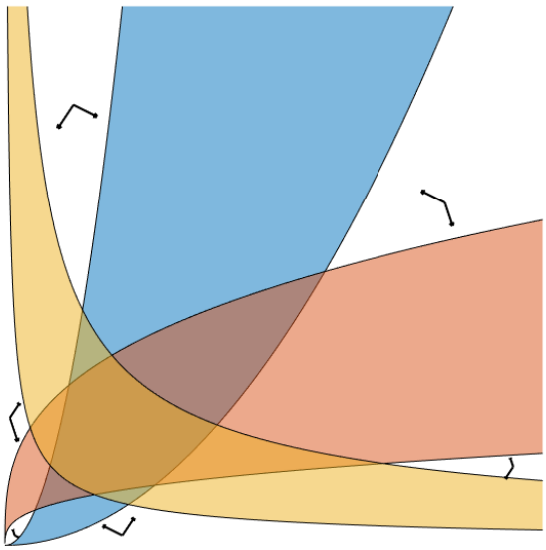

Figure 3.5: The fat curves in exponential space(toric differential inclusions).

Figure 3.6

The line regions in toric differential inclusions have the same width, while in variable-k dynamical systems the line regions have different width, but in variable-k dynamical systems the boundary of line regions go through two common points($(0, 2\ln\epsilon)$ and $(0, -2\ln\epsilon)$) on the y-axis.

In the toric differential inclusions, $\delta > 0$ is a constant. To apply the method in Chapter 4, δ must be a large positive number. When we are increasing δ the system will change as well, to analysis the difference in the picture one useful technique is re-scaling.

Example 3.2.1. We choose three line generators with slopes $\frac{1}{2}, 2$ and -1, first plot the figure when $\delta = 0.2$, then plot the figure when $\delta = 0.4$, if we change the measure to be the twice as in the first plot, the new figure will be similar to the first one. The linear part of

the figure will remain unchanged if we increase δ and xy coordinate in the same scale, as shown in below,

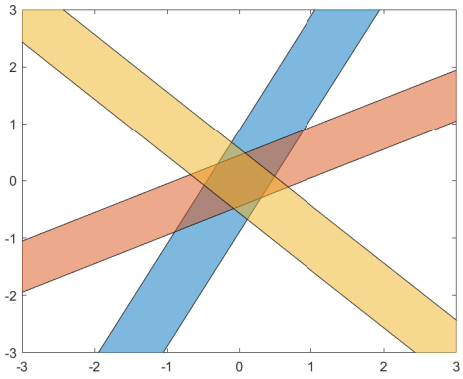

(a) The line regions in toric differential inclusions($\delta = 0.2$).

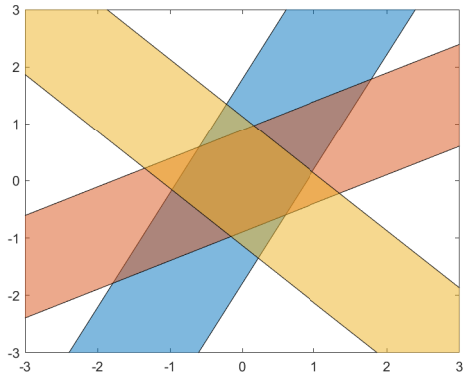

(b) The line regions in toric differential inclusions($\delta = 0.4$).

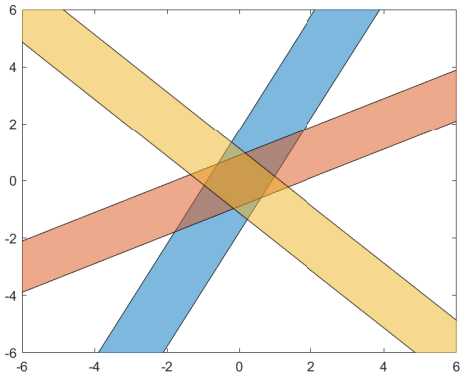

(c) The line regions in toric differential inclusions($\delta = 0.4$, after re-scaling).

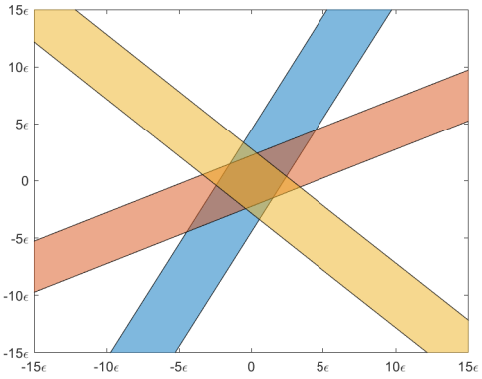

(d) The line regions in toric differential inclusions with arbitrary δ.

Figure 3.7: If we draw the coordinate by using δ like in (d), then the line regions will stay the same shape.

Proposition 3.2.2. *If the measure of the coordinates is proportional to δ, then the line regions will stay the same shape when we change δ.*

Proof. We can by calculate the boundary of the line regions. Let's prove the statement is true for the line region with the generator $px = qy$[1].

Since the line region is centered at origin with width 2δ, the upper and lower lines would be

$$\begin{aligned} y &= \frac{p}{q}x + \frac{\sqrt{p^2+q^2}}{q}\delta \\ y &= \frac{p}{q}x - \frac{\sqrt{p^2+q^2}}{q}\delta \end{aligned} \tag{3.2.1}$$

If x is proportional to δ, then $x = \delta t$, plug in to the previews equation we get

$$y = \delta(\frac{p}{q}t \pm \frac{\sqrt{p^2+q^2}}{q}) \tag{3.2.2}$$

So y is also proportional to δ, therefore we proved that the boundaries of line regions are always proportional to δ.

Moreover, as calculated in Chapter 4, the intersections of boundaries of line regions are also proportional to δ. If we increase δ to be $a\delta$ with $a > 1$, then the figure will expand in both x, y directions by multiplying with the parameter a we increase the measure of the coordinates also by a factor of a, then the figure will shrink in x, y directions by $\frac{1}{a}$, so in general the figure remains the same shape.

□

Example 3.2.3. Now we would show how the minimal invariant region and the minimal globally attracting region changes with δ in toric differential inclusions.

[1]We assume $q \neq 0$ in this case, when $q = 0$, the line is vertical to x-axis and we can prove the case with similar idea.

[2]

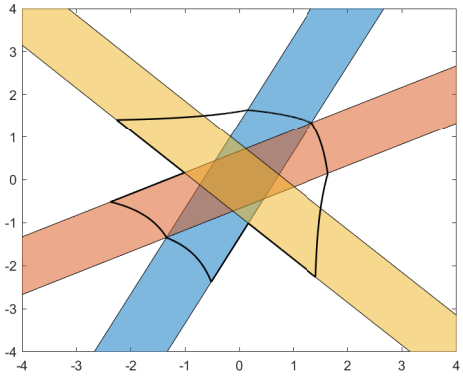

(a) The minimal invariant region in toric differential inclusions($\delta = 0.3$).

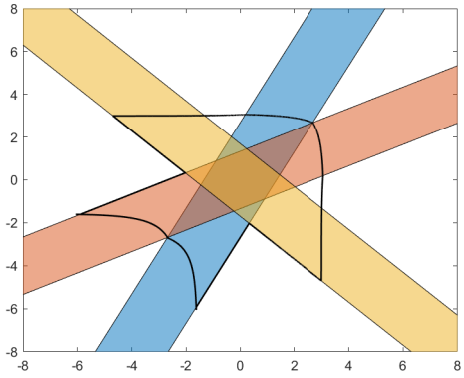

(b) The minimal invariant region in toric differential inclusions($\delta = 0.6$).

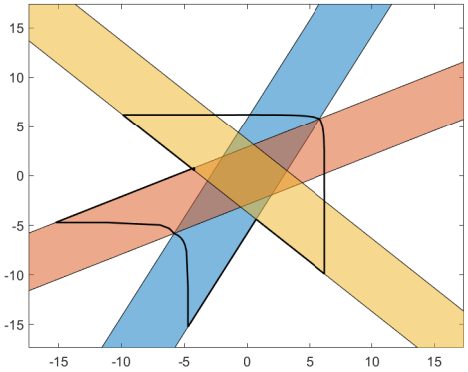

(c) The minimal invariant region in toric differential inclusions($\delta = 1.2$)

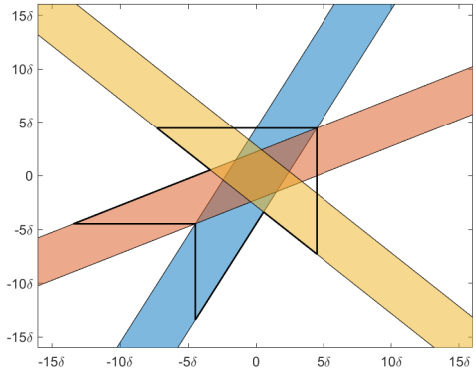

(d) The minimal invariant region in toric differential inclusions($\delta \to \infty$).

Figure 3.8: We can see that when δ is large, the minimal invariant region have very straight line segments, and the shape get to be like a 'fish'.

From this example, we can see that the graph and trajectories of solutions in mass-action systems tend to be straight lines in the logarithmic space if we rescale the graph properly. In the next section, we will discuss the behaviour of mass-action system in a

[2]In chapter 4 we will define the minimal invariant region in toric differential inclusions and we will give a method is construct the region in 2D.

logarithmic space when the scale of the coordinate is very large.

3.3 Mass action system in the large scale logarithmic space

Most of the lines and trajectories curves with bounded slope in the exponential space become almost vertical, almost horizontal or some parallel lines near $Y = X$ in a large scale logarithmic space.

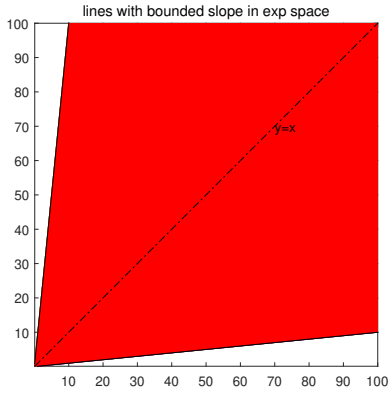

(a) The red cone region in the graph corresponds to the lines with bounded slope on $[\frac{1}{10}, 10]$ in the exponential space.

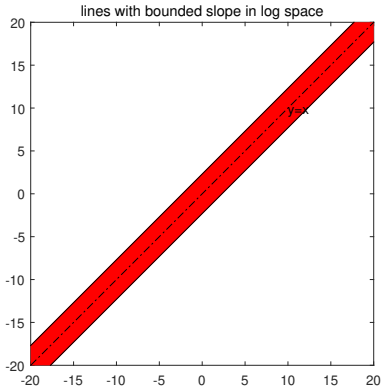

(b) The red stripes in the graph corresponds to the same lines in the logarithmic space.

Figure 3.9: bounded lines

The horizontal line $y = b_1$ and vertical line $x = b_2$ will remain to be horizontal lines $Y = \ln b_1$ and vertical lines $X = \ln b_2$. For all other kinds of line segments in the positive orthant in exponential space, the graph in logarithmic space have three possible shapes.

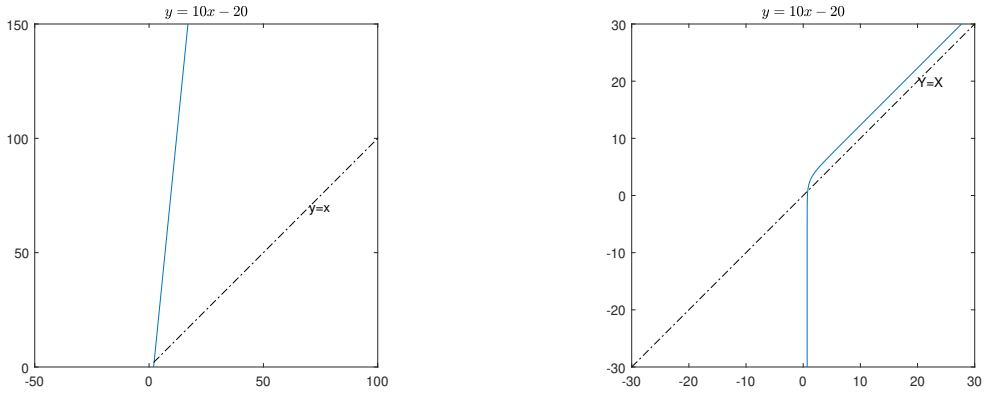

(a) (b)

Figure 3.10: The line regions in the exponential space and logarithmic space.(a)

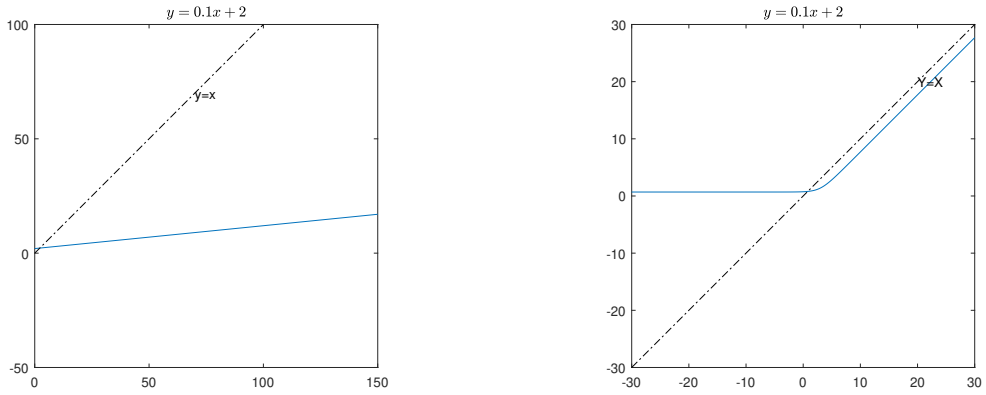

(a) (b)

Figure 3.11: The line regions in the exponential space and logarithmic space.(b)

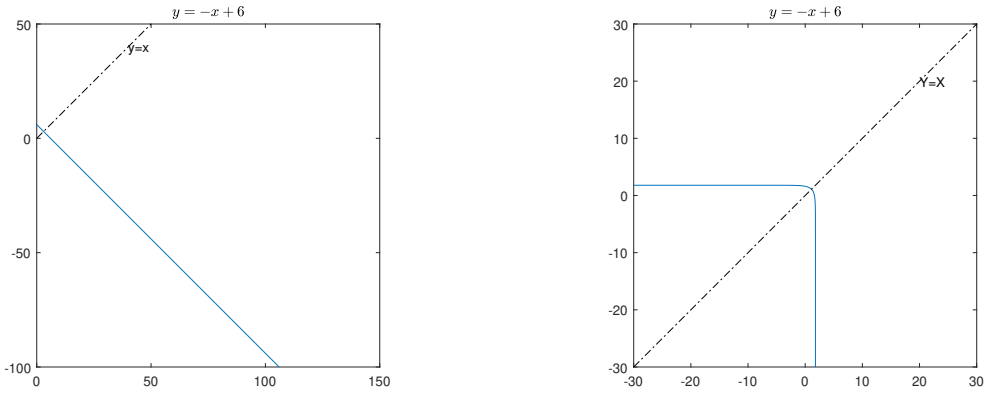

(a) (b)

Figure 3.12: The line regions in the exponential space and logarithmic space.(c)

Proposition 3.3.1. *In a large scale logarithmic space, all the line segments in the positive orthant $y = kx + b$ look like the three kinds of curves above. If $k > 0$ and $b < 0$ it looks like 3.10(b); If $k > 0$ and $b > 0$ it looks like 3.11(b); If $k < 0$ it looks like 3.12(b);*

Proof. Let's assume a line with nonzero slope k in the positive orthant,

$$y = kx + b \quad (x > 0,\ y > 0). \tag{3.3.1}$$

The corresponding coordinates in the logarithmic space are,

$$\begin{aligned} X &= \ln x \\ Y &= \ln y \end{aligned} \tag{3.3.2}$$

Then in the logarithmic space,

$$\begin{aligned} e^Y &= ke^X + b \\ Y' &= ke^{(X-Y)} = k\frac{x}{y} \end{aligned} \tag{3.3.3}$$

On the upper left half space of the line $Y = X$ in the logarithmic space while $x \to 0$,

$$x \to 0 \quad \Rightarrow \quad \frac{x}{y} \to 0 \quad \Rightarrow \quad Y' \to 0 \tag{3.3.4}$$

the figure looks like a horizontal line.

On the lower right half space of the line $Y = X$ in the logarithmic space while $y \to 0$,

$$y \to 0 \quad \Rightarrow \quad \frac{x}{y} \to \infty \quad \Rightarrow \quad Y' \to \infty \tag{3.3.5}$$

the figure looks like a vertical line. When $x \to \infty$

$$x \to \infty \quad \Rightarrow \quad \frac{x}{y} = \frac{x}{kx + b} \to \frac{1}{k} \quad \Rightarrow \quad Y' \to 1 \tag{3.3.6}$$

□

Remark 3.3.2. If the trajectory of a curve has its slope bounded in some intervals which do not contain 0, then from the starting point, the curve is bounded by two lines, which have the same behavior in the large scale logarithmic space, therefore, the curve will also have the similar shape as the figures we described above.

Chapter 4

Minimal invariant regions and minimal globally attracting regions for toric differential inclusions

4.1 Introduction

This chapter is structured as follows: In section 4.2, we present a procedure for constructing the minimal invariant region for a toric differential inclusion $\mathcal{T}_{\mathcal{F},\delta}$, which we denote by $\mathcal{M}_{\mathcal{F},\delta}$. In section 4.3, we give a proof of correctness for our procedure of constructing the minimal invariant region for a toric differential inclusion. In section 4.4, we show that the region $\mathcal{M}_{\mathcal{F},\delta}$ is also the minimal globally attracting region for a toric differential inclusion. We conclude by summarizing our results and give possible directions for future work.

4.2 Constructing $\mathcal{M}_{\mathcal{F},\delta}$

In what follows, we describe a procedure for the construction of $\mathcal{M}_{\mathcal{F},\delta}$ in the limit of large δ, where $\mathcal{F}$ is a hyperplane-generated complete polyhedral fan in $\mathbb{R}^2$. From here on, we will refer to a hyperplane-generated complete polyhedral fan in $\mathbb{R}^2$ simply as a fan. Moreover, to simplify the notation, we will denote a point $\boldsymbol{x} \in \mathbb{R}^2_{>0}$ by (x, y), and a point

$\boldsymbol{X} \in \mathbb{R}^2$ by (X, Y).

Let us denote the equations of the line generators of $\mathcal{F}$ by $q_i Y = p_i X$, where $1 \leq i \leq b$. We will consider lines that are parallel to these line generators and at a distance δ from them. Their equations are given by

$$\begin{aligned} q_i Y &= p_i X \pm \delta_i, \\ \text{where } \delta_i &= \delta \sqrt{p_i^2 + q_i^2}. \end{aligned} \tag{4.2.1}$$

Under the diffeomorphism $x = e^X, y = e^Y$, these lines get transformed to the curves

$$y^{q_i} = h_i x^{p_i}, \text{ where } h_i \in \{e^{-\delta_i}, e^{\delta_i}\}. \tag{4.2.2}$$

We will call the region bounded between the curves $y^{q_i} = e^{-\delta_i} x^{p_i}$ and $y^{q_i} = e^{\delta_i} x^{p_i}$ the *uncertainty region* corresponding to the line $q_i Y = p_i X$.

Remark 4.2.1. Consider a fan $\mathcal{F}$. Then the point $(1, 1)$ is contained in the interior of every uncertainty region of $\mathcal{F}$.

Proof. Consider a line generator of $\mathcal{F}$ given by $q_i Y = p_i X$. The uncertainty region corresponding to this line generator is the area bounded between the curves $y^{q_i} = e^{-\delta_i} x^{p_i}$ and $y^{q_i} = e^{\delta_i} x^{p_i}$. Note that $1 \in (e^{-\delta_i}, e^{\delta_i})$. Therefore, the point $(1, 1)$ belongs to the interior of the uncertainty region corresponding to the line $q_i Y = p_i X$. Since our choice of the uncertainty region was arbitrary, we get that $(1, 1)$ is in the interior of every uncertainty region of $\mathcal{F}$. □

Lemma 4.2.2. *Consider the fans $\mathcal{F}$ and $\tilde{\mathcal{F}}$ such that the set of line generators of $\tilde{\mathcal{F}}$ are*

contained in the set of line generators of $\mathcal{F}$*. Then, we have* $\mathcal{T}_{\tilde{\mathcal{F}},\delta} \subseteq \mathcal{T}_{\mathcal{F},\delta}$*, i.e.,* $F_{\tilde{\mathcal{F}},\delta}(\boldsymbol{X}) \subseteq F_{\mathcal{F},\delta}(\boldsymbol{X})$ *for every* $\boldsymbol{X} \in \mathbb{R}^n$*.*

Proof. Let $\boldsymbol{X} \in \mathbb{R}^n$. From Equation (2.3.6), we have

$$F_{\mathcal{F},\delta}(\boldsymbol{X}) = \left(\bigcap_{\substack{C \in \mathcal{F} \\ dist(\boldsymbol{X},C) \leq \delta \\ dim(C)=n}} C \right)^o, \tag{4.2.3}$$

and

$$F_{\tilde{\mathcal{F}},\delta}(\boldsymbol{X}) = \left(\bigcap_{\substack{\tilde{C} \in \tilde{\mathcal{F}} \\ dist(\boldsymbol{X},\tilde{C}) \leq \delta \\ dim(\tilde{C})=n}} \tilde{C} \right)^o. \tag{4.2.4}$$

Let $dist(\boldsymbol{X}, C) \leq \delta$ for some $C \in \mathcal{F}$ such that $dim(C) = n$. Then, because the set of line generators of $\tilde{\mathcal{F}}$ are contained in the set of line generators of $\mathcal{F}$, there exists a unique cone $\tilde{C} \in \tilde{\mathcal{F}}$ with $dim(\tilde{C}) = n$ such that $C \subseteq \tilde{C}$. Since $C \subseteq \tilde{C}$ and $dist(\boldsymbol{X}, C) \leq \delta$, we have $dist(\boldsymbol{X}, \tilde{C}) \leq \delta$. In addition, if $dist(\boldsymbol{X}, C'') \leq \delta$ for some $C'' \in \tilde{\mathcal{F}}$ with $dim(C'') = n$, then there exists atleast one $C' \in \mathcal{F}$ such that $C' \subseteq C'', dim(C') = n$ and $dist(\boldsymbol{X}, C') \leq \delta$. This is true because if $dist(\boldsymbol{X}, \hat{C}) > \delta$ for every $\hat{C} \in \mathcal{F}$ such that $\hat{C} \subseteq C$ and $dim(\hat{C}) = n$, then since

$$C'' = \bigcup_{\substack{\hat{C} \subseteq C'' \\ dim(\hat{C})=n}} \hat{C} \tag{4.2.5}$$

we get $dist(\boldsymbol{X}, C'') > \delta$, a contradiction. This implies that

$$\bigcap_{\substack{C\in\mathcal{F}\\ dist(\boldsymbol{X},C)\leq\delta\\ dim(C)=n}} C \subseteq \bigcap_{\substack{\tilde{C}\in\tilde{\mathcal{F}}\\ dist(\boldsymbol{X},\tilde{C})\leq\delta\\ dim(\tilde{C})=n}} \tilde{C}. \tag{4.2.6}$$

Since our choice of the point $\boldsymbol{X}$ was arbitrary, it follows that

$$F_{\tilde{\mathcal{F}},\delta}(\boldsymbol{X}) \subseteq F_{\mathcal{F},\delta}(\boldsymbol{X}) \tag{4.2.7}$$

for every $\boldsymbol{X} \in \mathbb{R}^n$, as desired. □

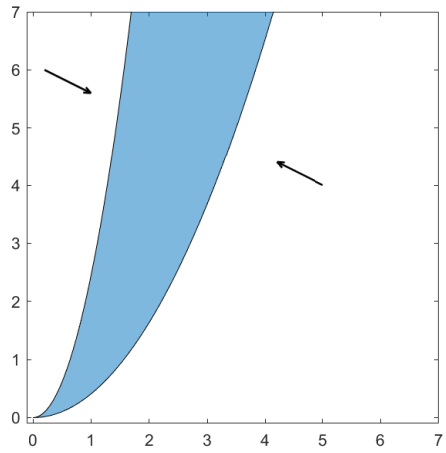

Figure 4.1: Attracting directions(shown in black) corresponding to an uncertainty region(shown in blue).

Definition 4.2.3 (Attracting directions)**.** Consider a fan $\mathcal{F}$. Let UC be the uncertainty region corresponding to a line generator $qY = pX$ of $\mathcal{F}$. The complement of UC given by $\mathbb{R}^2_{>0} \setminus UC$ consists of two connected components. We define the **attracting directions** of UC to be the directions that are orthogonal to the line $qY = pX$ and point towards the uncertainty region UC within each connected component.

Figure 4.1 shows the attracting directions corresponding to an uncertainty region.

Definition 4.2.4. Consider a fan $\mathcal{F}$ and the uncertainty regions corresponding to its one-dimensional generators. Given $\boldsymbol{x} \in \mathbb{R}^2_{>0}$, we define $r(\boldsymbol{x})$ to be the number of uncertainty regions that contain the point $\boldsymbol{x}$ in their interior.

In the next remark, we relate the right-hand side of the toric differential inclusion on $\mathbb{R}^2_{>0}$ with the function $r(\boldsymbol{x})$.

Remark 4.2.5. The toric differential inclusion $\frac{d\boldsymbol{x}}{dt} \in F_{\mathcal{F},\delta}(\boldsymbol{X})$ can be described as follows:

(i) If $r(\boldsymbol{x}) = 1$, and $\boldsymbol{x}$ is in the uncertainty region corresponding to the line $q_iY = p_iX$. If $p_iY + q_iX \geq 0$, then the cone $F_{\mathcal{F},\delta}(\boldsymbol{X})$ is the half space $p_iY + q_iX \geq 0$. If $p_iY + q_iX \leq 0$, then the cone $F_{\mathcal{F},\delta}(\boldsymbol{X})$ is the half space $p_iY + q_iX \leq 0$.

(ii) If $r(\boldsymbol{x}) \geq 2$, then $F_{\mathcal{F},\delta}(\boldsymbol{X}) = \mathbb{R}^2$.

(iii) If $r(\boldsymbol{x}) = 0$, and $\boldsymbol{x}$ lies in the region between the two nearest uncertainty regions which correspond to the lines $q_iY = p_iX$ and $q_jY = p_jX$. Then $F_{\mathcal{F},\delta}(\boldsymbol{X})$ is a proper cone formed by the intersection of two half-spaces which are the right-hand sides of the toric differential inclusion corresponding to these two uncertainty regions.

Assumption 4.2.6. We will assume that the fan $\mathcal{F}$ has at least one line generator having slope > 1, at least one line generator having slope such that $0 < slope < 1$ and at least one line generator having slope < 0. In addition, we will assume that the line generators of the fan do not have zero or infinite slope. These special cases will be dealt in Section 4.5.

To build the region $\mathcal{M}_{\mathcal{F},\delta}$, we use the following steps:

Step 1: Calculate the intersections of uncertainty regions

One can calculate the coordinates corresponding to the intersection of uncertainty regions by solving the following system of equations

$$\begin{aligned} y^{q_i} &= e^{\pm\delta_i} x^{p_i}, \\ y^{q_j} &= e^{\pm\delta_j} x^{p_j} \end{aligned} \tag{4.2.8}$$

for every $i \neq j$. Solving them gives us the following points

$$\begin{aligned} &(x_1, y_1) = \left(e^{\frac{q_i\delta_j - q_j\delta_i}{p_iq_j - p_jq_i}}, e^{\frac{p_i\delta_j - p_j\delta_i}{p_iq_j - p_jq_i}} \right), (x_2, y_2) = \left(e^{\frac{q_i\delta_j + q_j\delta_i}{p_iq_j - p_jq_i}}, e^{\frac{p_i\delta_j + p_j\delta_i}{p_iq_j - p_jq_i}} \right), \\ &(x_3, y_3) = \left(e^{\frac{-q_i\delta_j - q_j\delta_i}{p_iq_j - p_jq_i}}, e^{\frac{-p_i\delta_j - p_j\delta_i}{p_iq_j - p_jq_i}} \right), (x_4, y_4) = \left(e^{\frac{-q_i\delta_j + q_j\delta_i}{p_iq_j - p_jq_i}}, e^{\frac{-p_i\delta_j + p_j\delta_i}{p_iq_j - p_jq_i}} \right). \end{aligned} \tag{4.2.9}$$

Remark 4.2.7. Note that substituting $\delta_i = \delta\sqrt{p_i^2 + q_i^2}, \delta_j = \delta\sqrt{p_j^2 + q_j^2}$ from Equation (4.2.1) into Equation (4.2.9), we get that the intersection points of the uncertainty regions can be parametrised as $(x, y) = (e^{C\delta}, e^{D\delta})$, where $C = f(p_i, p_j, q_i, q_j)$ and $D = g(p_i, p_j, q_i, q_j)$ for some appropriate functions f and g.

Let us denote by S^{uc} the set of all possible intersection points between the uncertainty regions. Let us assume that the fan $\mathcal{F}$ has line generators given by the set $\mathcal{L} = \{q_iY = p_iX \mid i \in [b]\}$, where $[b] = \{1, 2, ..., b\}$. We can classify the uncertainty regions into the following groups. Let $S_1 = \{i \in [b] \mid \frac{p_i}{q_i} < 0\}, S_2 = \{i \in [b] \mid \frac{p_i}{q_i} > 0,\ |q_i| > |p_i|\}, S_3 = \{i \in [b] \mid \frac{p_i}{q_i} > 0,\ |q_i| \leq |p_i|\}$. Note that by assumption 4.2.6, each of the sets S_1, S_2, S_3

is non-empty. Define

$$\begin{aligned} i_1 &= \arg\max_{i \in S_1} \frac{p_i}{q_i} \\ i_2 &= \arg\min_{i \in S_2} \frac{p_i}{q_i} \\ i_3 &= \arg\max_{i \in S_3} \frac{p_i}{q_i} \\ i_4 &= \arg\min_{i \in S_1} \frac{p_i}{q_i} \end{aligned} \tag{4.2.10}$$

Figure 4.2 shows the uncertainty regions of the fan $\mathcal{F}$.

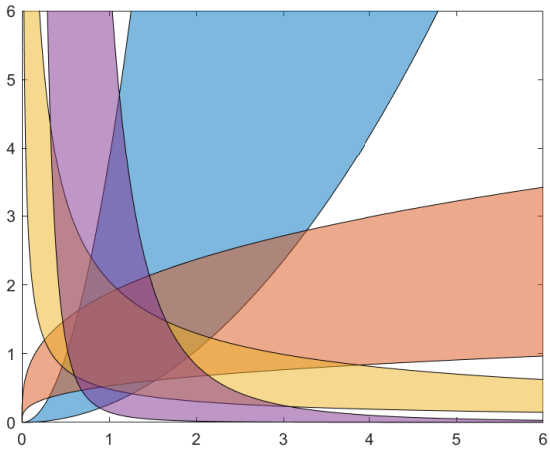

Figure 4.2: Plot depicting the uncertainty regions of the fan $\mathcal{F}$.

Step 2: Choose (N, M) ***and*** (n, m)***, the starting points for constructing*** $M_\delta^{\mathcal{F}}$

Let $S^{\text{uc}} = \{(x_1, y_1), (x_2, y_2), ..., (x_p, y_p))\}$ denote the set of intersection points of the uncertainty regions. Let $x_{\max} = \max_{1 \le i \le p} x_i$ and $y_{\max} = \max_{1 \le i \le p} y_i$. Let us assume that $y_{\max} = \max(x_{\max}, y_{\max})$. We will set $M = y_{\max}$ and will denote the intersection point in S^{uc} whose y coordinate is M by (N, M)[1].

[1]If we have several points with same maximal value like (N_1, M), (N_2, M), ..., then choose the intersection

Let $m = \min(\max(x_1, y_1), \max(x_2, y_2), ..., \max(x_p, y_p))$. We will denote the intersection point in S^{uc} with this coordinate by (n, m). These two points will serve as the starting points for building the region $\mathcal{M}_{\mathcal{F},\delta}$. Figure 4.3 illustrates this point.

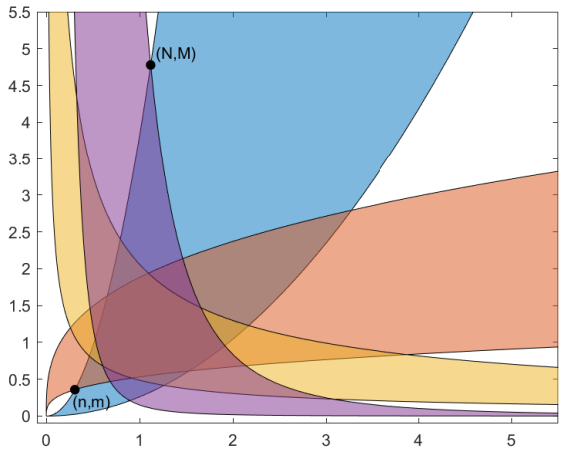

Figure 4.3: Choose starting points (N, M) and (n, m)

Step 3: Starting from (N, M) ***build polygonal lines*** I_1, I_4**.**

The procedure described in this step is with respect to Figure 4.4. Starting from $A_0 = (N, M)$, we build the polygonal line in a counter-clockwise sense as follows. The first line segment that we build is A_0A_1 that crosses an uncertainty region such that its slope is given by the slope of the attracting direction of this uncertainty region. Then starting at A_1, we repeat this process until one reaches the outer boundary of the uncertainty region with index i_1. We will denote these trajectories of polygonal lines by I_1.

Then starting from $A_0 = (N, M)$ again, we build the polygonal line in a clockwise sense as follows. The first line segment that we build is A_0B_1 that crosses an uncertainty

point closest to the line $y = x$.

region such that its slope is given by the slope of the attracting direction of this uncertainty region. Then starting at B_1, we repeat this process until one reaches the outer boundary of the uncertainty region with index i_4. We will denote these trajectories of polygonal lines by I_4.

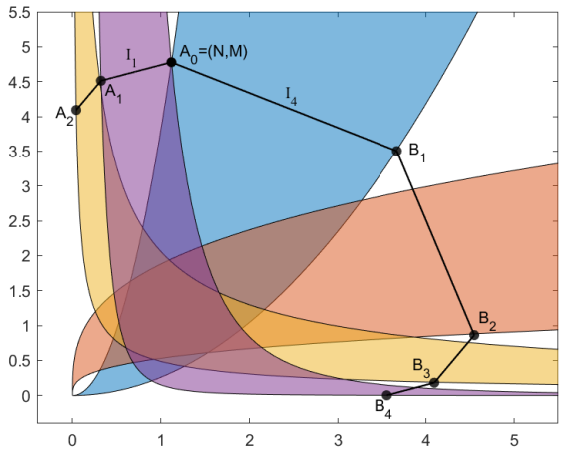

Figure 4.4: Build polygonal lines I_1, I_4

Step 4: Starting from (n, m) ***build polygonal lines*** I_2, I_3

The procedure described in this step is with respect to Figure 4.5. Starting from $C_0 = (n, m)$, we build the polygonal line in a clockwise sense as follows. The first line segment that we build is C_0C_1 that crosses an uncertainty region such that its slope is given by the slope of the attracting direction of this uncertainty region. Then starting at C_1, we repeat this process until one reaches the outer boundary of the uncertainty region with index i_2. We will denote these trajectories of polygonal lines by I_2.

Then starting from $C_0 = (n, m)$ again, we build the polygonal line in a counter-clockwise sense as follows. The first line segment that we build is C_0D_1 that crosses an uncertainty region such that its slope is given by the slope of the attracting direction of

this uncertainty region. Then starting at D_1, we repeat this process until one reaches the outer boundary of the uncertainty region with index i_3. We will denote these trajectories of polygonal lines by I_3.

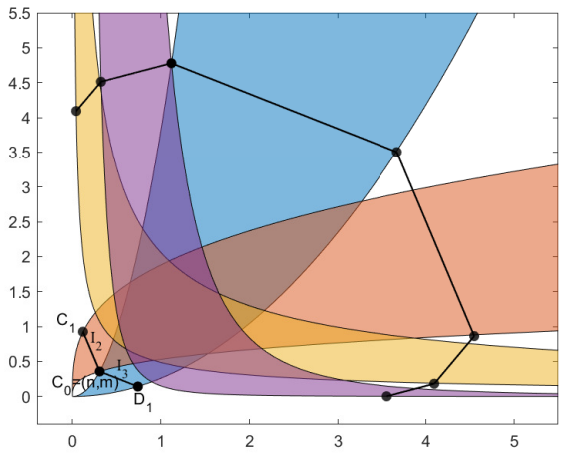

Figure 4.5: Build polygonal lines I_2, I_3

Step 5: Connect I_1, I_2, I_3, I_4

We will connect I_1 and I_2 by following the curves $\mathcal{C}_{i_1}$, $\mathcal{C}_{i_2}$ and will connect I_3 and I_4 by following the curves $\mathcal{C}_{i_3}, \mathcal{C}_{i_4}$ as shown in Figure 4.6. This gives us the boundary of $\mathcal{M}_{\mathcal{F},\delta}$.

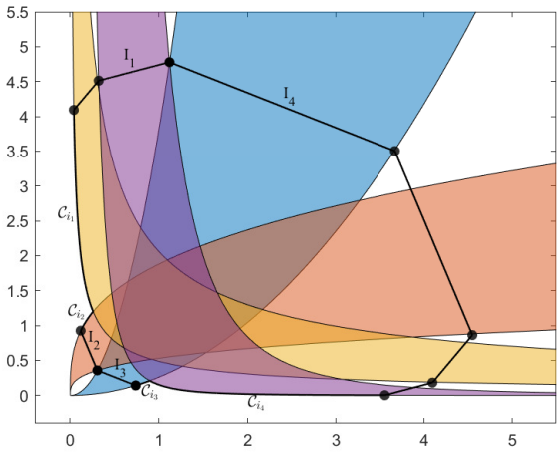

Figure 4.6: Connect I_1, I_2, I_3, I_4

4.3 The minimal invariant region

We will assume the following notation with respect to the construction of $M_\delta^{\mathcal{F}}$ for the rest of the paper.

- Let $C_\delta^{\mathcal{F}}$ denote the boundary of $M_\delta^{\mathcal{F}}$.
- The line segments in $C_\delta^{\mathcal{F}}$ can be decomposed into the following paths:

  (i) $\{B_u, B_{u-1}, \cdots, B_p, B_{p-1}, \cdots, B_1, A_0 = (N, M), A_1, A_2 \cdots, A_q\}$.

  (ii) $\{C_r, C_{r-1} \cdots, C_1, C_0 = (n, m), D_1, D_2, \cdots, D_s\}$,

  where A_q is the terminal point in the construction of I_1 and lies on the uncertainty region with index i_1, B_u is the terminal point in the construction of I_4 and lies on the uncertainty region with index i_4, C_r is the terminal point in the construction of I_2 and lies on the uncertainty region with index i_2 and D_s is the terminal point in the

construction of I_3 and lies on the uncertainty region with index i_3. Figure 4.7 shows these points.

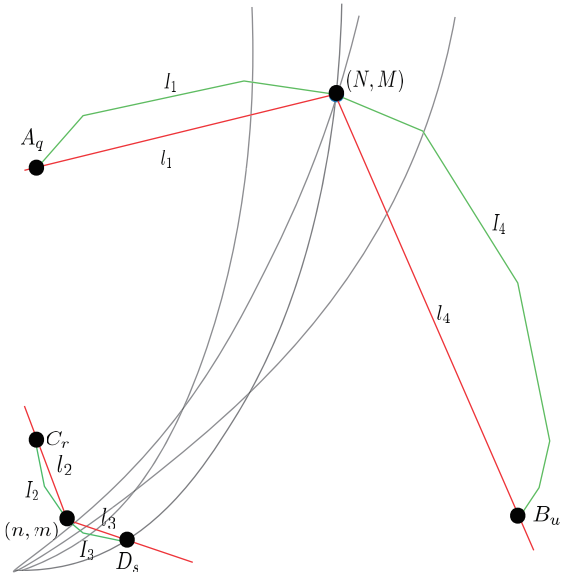

Figure 4.7: The green polygonal line denotes the paths I_1, I_2, I_3, I_4. The line segments l_1, l_2, l_3, l_4 are marked in red. The cone C_{l_1,l_4} is formed by the line segments l_1 and l_4 with vertex at (N, M). The cone C_{l_2,l_3} is formed by the line segments l_2 and l_3 with vertex at (n, m).

- We will denote the following

  l_1: line segment connecting (N, M) to A_q.

  l_2: line segment connecting (n, m) to C_r.

  l_3: line segment connecting (n, m) to D_s.

  l_4: line segment connecting (N, M) to B_u.

  C_{l_1,l_4}: cone formed by the line segments l_1 and l_4 with vertex at (N, M).

  C_{l_2,l_3}: cone formed by the line segments l_2 and l_3 with vertex at (n, m).

Figure 4.7 illustrates the cones C_{l_1,l_4} and C_{l_2,l_3} formed by the line segments l_1, l_2, l_3, l_4.

Remark 4.3.1. Let us denote the coordinates of the point B_u in the construction of $M_\delta^{\mathcal{F}}$ as (x_u, y_u). By assumption 4.2.6, there is at least one line generator having negative slope and at least one line generator have positive slope. Since B_u is the terminal point in the construction of I_4, it lies in the fourth quadrant with respect to Figure 4.8. The point M has the maximum coordinate among the points in S^{uc} and therefore lies either in the first or the second quadrant with respect to Figure 4.8. This implies that $\log(M) > 0$ and $\log(y_u) < 0$ or equivalently $M > 1$ and $y_u < 1$.

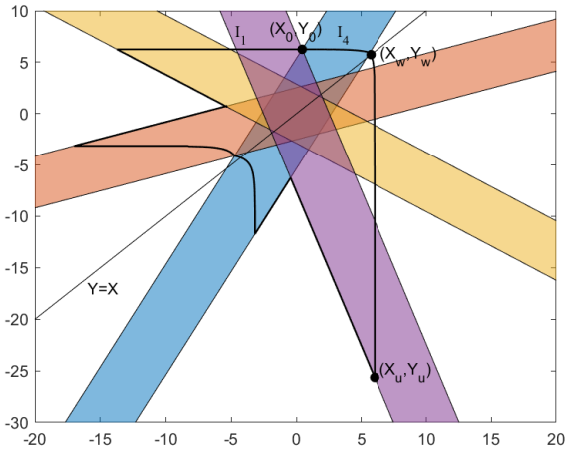

Figure 4.8: The curve $C_\delta^{\mathcal{F}}$ in logarithmic space.

Remark 4.3.2. It is instructive to visualize the line segments of $C_\delta^{\mathcal{F}}$ in logarithmic space. In particular, consider the diffeomorphism $\phi : (x, y) \to (X, Y)$, where $X = \log(x), Y = \log(y)$. The Jacobian of this diffeomorphism is $J = \begin{pmatrix} e^{-X} & 0 \\ 0 & e^{-Y} \end{pmatrix}$. For $Y - X \gg 1$, we consider the rescaled Jacobian $J_1 = \begin{pmatrix} e^{Y-X} & 0 \\ 0 & 1 \end{pmatrix}$. For $X - Y \gg 1$, we consider the rescaled Jacobian

$$J_2 = \begin{pmatrix} 1 & 0 \\ 0 & e^{X-Y} \end{pmatrix}.$$

Note that for $M > N$ and δ large enough, the rescaled Jacobians J_1 and J_2 show that the path I_4 consists of an (almost) horizontal component and an (almost) vertical component separated by the line $Y = X$ in logarithmic space. Figure 4.8 illustrates this fact. Since we assumed δ to be very large, the shape of I_4 in the narrow region around $Y = X$ can be safely ignored.

Lemma 4.3.3. *Consider the path I_4 that starts from the point (N, M) in the construction of $M_\delta^{\mathcal{F}}$. Let us denote the coordinates of the terminal point B_u on I_4 by (x_u, y_u). If $N < M$, then in the limit of large δ, we have $x_u = O(M)$.*

Proof. Let us denote the coordinates of (N, M) by (x_0, y_0) and let (x_w, y_w) be the intersection of I_4 with the line $y = x$. Our proof will proceed by analysing the following paths along I_4: (i) From (x_0, y_0) to (x_w, y_w) and (ii) From (x_w, y_w) to (x_u, y_u). Let Q denote the set of slopes of the line segments on the path I_4 starting from (x_0, y_0) to (x_w, y_w). Now consider the line connecting (x_0, y_0) to (x_w, y_w). Let Q_{min} and Q_{max} denote the minimum and maximum slopes in the set Q. Then we have $y_w - y_0 = \bar{s}(x_w - x_0)$, where $Q_{\min} \leq \bar{s} \leq Q_{max}$ and $\bar{s} \neq 1$. By remark 4.2.7, we know that the point (x_0, y_0) can be parametrized as $(x_0, y_0) = (e^{N'\delta}, e^{M'\delta})$ for some $N', M' \in \mathbb{R}$. Since $x_w = y_w$, we get $y_w - e^{M'\delta} = \bar{s}(y_w - e^{N'\delta})$. This gives

$$y_w = \frac{1}{1-\bar{s}}(e^{M'\delta} - \bar{s}e^{N'\delta}). \tag{4.3.1}$$

Without loss of generality, assume that $y_w = h(x, y, \delta)e^{M'\delta}$ for some function $h(x, y, \delta)$. Inserting this expression of y_w into Equation (4.3.1), we get

$$h(x, y, \delta) = \frac{1}{1-\bar{s}}(1 - \bar{s}e^{(N'-M')\delta}) \to \frac{1}{1-\bar{s}} \text{ as } \delta \to \infty. \tag{4.3.2}$$

, where the last step follows because $M > N$ or equivalently $M' > N'$. Therefore, $h(x, y, \delta)$ approaches a bounded constant as $\delta \to \infty$. This implies that $x_w = y_w = O(M)$.

Now consider the path along I_4 from (x_w, y_w) to (x_u, y_u). Let Q' denote the set of slopes of the line segments on this path. Consider the line connecting (x_w, y_w) to (x_u, y_u). Let Q'_{min} and Q'_{max} denote the minimum and maximum slopes in the set Q'. Then we have $y_w - y_u = \tilde{s}(x_w - x_u)$, where $Q'_{min} \leq \tilde{s} \leq Q'_{max}$ and $\tilde{s} \neq 1$. Note that since $y_w \neq y_u$, we have $\tilde{s} \neq 0$. Further, since $x_w = y_w$, we have $x_w - y_u = \tilde{s}(x_w - x_u)$. This gives

$$x_w = \frac{1}{1 - \tilde{s}}(y_u - \tilde{s}x_u). \tag{4.3.3}$$

Let us assume that $x_w = \tilde{h}(x, y, \delta)x_u$ for some function $\tilde{h}(x, y, \delta)$. Inserting this expression of x_w into Equation (4.3.3), we get

$$\tilde{h}(x, y, \delta) = \frac{1}{1 - \tilde{s}}\left(\frac{y_u}{x_u} - \tilde{s}\right) \tag{4.3.4}$$

Note from remark 4.3.2 that if $M > N$ and for δ large enough, the path I_4 consists of an (almost) horizontal component and an (almost) vertical component separated by the line $Y = X$ in logarithmic space. This implies that $\log(x_u) > \log(y_u)$ or equivalently $x_u > y_u$. Note that $\tilde{h}(x, y, \delta) > 0$ for all $x, y \in \mathbb{R}^2_{>0}$ and $\delta > 0$. Therefore, we have

$$\tilde{h}(x, y, \delta) = \left|\frac{1}{1 - \tilde{s}}\right|\left|\frac{y_u}{x_u} - \tilde{s}\right| \leq \left|\frac{1}{1 - \tilde{s}}\right|\left(\left|\frac{y_u}{x_u}\right| + |\tilde{s}|\right) < \left|\frac{1}{1 - \tilde{s}}\right|(1 + |\tilde{s}|). \tag{4.3.5}$$

This shows that $\tilde{h}(x, y, \delta)$ is upper bounded by a constant. We now show that $\tilde{h}(x, y, \delta)$ is lower bounded by a constant. Consider the following cases:

- $\tilde{s} > 1$: Since $\frac{y_u}{x_u} < 1$, we get that $\tilde{h}(x, y, \delta) = \frac{1}{1-\tilde{s}}\left(\frac{y_u}{x_u} - \tilde{s}\right) > 1$.

- $0 < \tilde{s} < \frac{y_u}{x_u} < 1$: We show that this case cannot happen. Consider the triangle formed by the points $(0,0), (x_u, y_u), (x_w, y_w)$. The slope of the line segment joining $(0,0)$ to (x_u, y_u) has slope $\frac{y_u}{x_u}$ which is less than 1. In addition, the slope of the line segment joining (x_u, y_u) to (x_w, y_w) has slope $\tilde{s}$ which is less than 1. This implies that the slope of the line segment joining $(0,0)$ to (x_w, y_w) is less than 1, contradicting the fact $x_w = y_w$.

- $\tilde{s} < 0 < \frac{y_u}{x_u} < 1$: Since $\frac{y_u}{x_u} > 0$, we get that $\tilde{h}(x, y, \delta) = \frac{1}{1-\tilde{s}}\left(\frac{y_u}{x_u} - \tilde{s}\right) > \frac{-\tilde{s}}{1-\tilde{s}}$.

Since $\tilde{h}(x, y, \delta)$ is upper bounded and lower bounded by some constants, we get that $x_u = O(x_w) = O(M)$.

□

We assume a certain ordering on the uncertainty regions of a fan by looking at the corresponding picture in logarithmic space. The uncertainty region corresponding to the line having the minimum positive slope has index 1. The uncertainty region corresponding to the line having the minimum negative slope has the highest index. The intermediate indices of the uncertainty regions are assigned in increasing order in the counter-clockwise sense. Figure 4.9 illlustrates this point.

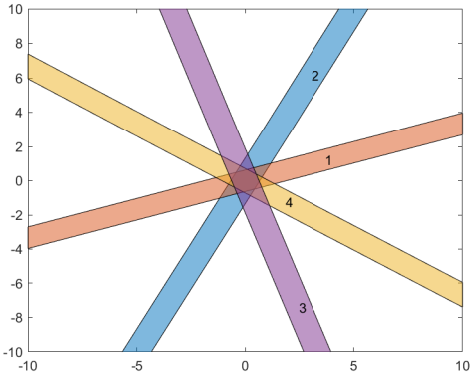

(a) Fan with strips of width δ drawn around its line generators.

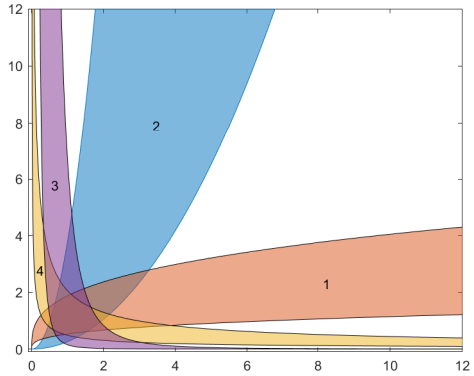

(b) This figure is obtained by exponentiating the lines in Figure 4.9(a).

Figure 4.9: We choose a natural ordering on the fat lines in Figure 4.9(a) starting from the line of the smallest positive slope to the line of the smallest negative slope in a counter-clockwise sense. This induces a corresponding ordering on the uncertainty regions as depicted in Figure 4.9(b). The notion of going along the attracting direction of the next uncertainty region implies that we traverse the uncertainty regions in a certain order. This in turn induces an ordering on the slopes of the attracting directions along our path, which is the idea behind remark 4.3.4.

Remark 4.3.4. Note that the construction of $M_\delta^{\mathcal{F}}$ proceeds by building line segments that go in the attracting direction of the next uncertainty region starting from the points $A_0 = (N, M)$ and $C_0 = (n, m)$. This puts a natural order on the slopes of the line segments that constitute $M_\delta^{\mathcal{F}}$, as remarked in the caption of Figure 4.9. In particular, let B_p be the point in the construction of I_4 with the maximum x-coordinate. Then, we have the following:

- $slope(l_{B_p,B_{p-1}}) < \cdots < slope(l_{B_1,A_0}) < slope(l_{A_0,A_1}) < \cdots < slope(l_{A_{q-1},A_q})$.
- $slope(l_{C_r,C_{r-1}}) < \cdots < slope(l_{C_1,C_0}) < slope(l_{C_0,D_1}) < \cdots < slope(l_{D_{s-1},D_s}) < 0$.
- $0 < slope(l_{B_u,B_{u-1}}) < \cdots < slope(l_{B_{p+1},B_p})$.

Lemma 4.3.5. *The cone corresponding to the right-hand side of the toric differential inclusion $\mathcal{T}_{\mathcal{F},\delta}$ at any point on the curves $\mathcal{C}_{i_1}, \mathcal{C}_{i_2}, \mathcal{C}_{i_3}, \mathcal{C}_{i_4}$ is contained in the interior of the uncertainty regions of these curves.*

Proof. We will present a proof for the case of $\mathcal{C}_{i_1}$ and $\mathcal{C}_{i_2}$, the case of $\mathcal{C}_{i_3}$ and $\mathcal{C}_{i_4}$ will follow analogously. Let us denote the intersection point of $\mathcal{C}_{i_1}$ and $\mathcal{C}_{i_2}$ by P_{i_1,i_2}. We now show the following:

- The slopes of the tangents to the curve starting from the point A_q increase monotonically along the curve until the point P_{i_1,i_2}. To see this, note that since we stop building line segments in the construction of $M_\delta^{\mathcal{F}}$ at the uncertainty region with index i_1, Equation (4.2.2) gives us that $\mathcal{C}_{i_1}$ lies on the curve of the form $y^q = e^{-\sqrt{p^2+q^2}\delta}x^p$, where p and q are such that $p < 0$ and $q > 0$. Differentiating the equation of the curve $\mathcal{C}_{i_1}$, we get

$$y' = \frac{p}{q} y^{(1-\frac{q}{p})} e^{\frac{-\sqrt{p^2+q^2}\delta}{p}} \tag{4.3.6}$$

  Therefore, the slope of the tangent to the curve $\mathcal{C}_{i_1}$ increases with decrease in y and the desired conclusion follows.

- The slopes of the tangents to the curve starting from the point C_r decrease monotonically along the curve until the point P_{i_1,i_2}. To see this, note that since we stop building line segments in the construction of $M_\delta^{\mathcal{F}}$ at the uncertainty region with index i_2, Equation (4.2.2) gives us that $\mathcal{C}_{i_2}$ lies on the curve of the form $y^{\tilde{q}} = e^{\sqrt{\tilde{p}^2+\tilde{q}^2}\delta}x^{\tilde{p}}$, where $\tilde{p} > 0, \tilde{q} > 0$ and $\frac{\tilde{q}}{\tilde{p}} > 1$. Differentiating the equation of the curve $\mathcal{C}_{i_2}$, we get

$$y' = \frac{\tilde{p}}{\tilde{q}} y^{(1-\frac{\tilde{q}}{\tilde{p}})} e^{\frac{\sqrt{\tilde{p}^2+\tilde{q}^2}\delta}{\tilde{p}}} \tag{4.3.7}$$

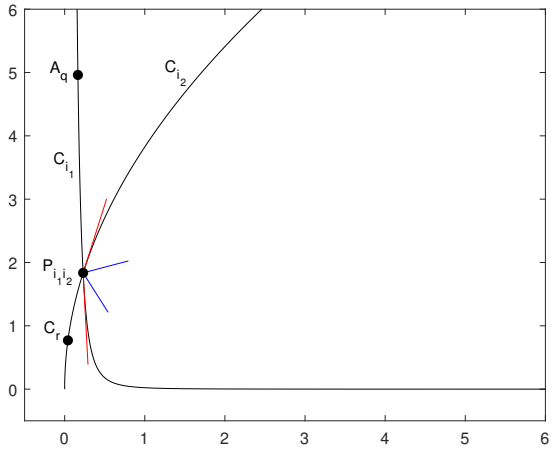

Figure 4.10: The right-hand side of the toric differential inclusion $\mathcal{T}_{\mathcal{F},\delta}$ evaluated at the point P_{i_1,i_2} (denoted by the blue cone) is contained in the red cone formed by the tangents to the curves $\mathcal{C}_{i_1}$ and $\mathcal{C}_{i_2}$ at the point P_{i_1,i_2}.

Therefore, the slope of the tangent to the curve $\mathcal{C}_{i_2}$ decreases with increase in y and we are done.

Consider Figure 4.10, which shows a sketch of the regions $\mathcal{C}_{i_1}$ and $\mathcal{C}_{i_2}$. Due to the monotonicity of the slopes of the tangents to $\mathcal{C}_{i_1}$ and $\mathcal{C}_{i_2}$ as argued above, it suffices to show that the cone corresponding to the right-hand side of $\mathcal{T}_{\mathcal{F},\delta}$(marked in blue) lies inside the cone formed by the tangents to the curves $\mathcal{C}_{i_1}$ and $\mathcal{C}_{i_2}$ at the point P_{i_1,i_2}(marked in red). Note that from Equations (4.3.6) and (4.3.7), we get that $|y'| \to \infty$ as $\delta \to \infty$. Therefore, the slopes of the generators of the red cone can be made as large as possible so that it contains the cone corresponding to the right-hand side of $\mathcal{T}_{\mathcal{F},\delta}$.

□

Lemma 4.3.6. *The line segments l_1, l_2, l_3, l_4 lie inside $M_\delta^{\mathcal{F}}$.*

Proof. We will first show that l_1 lies inside $M_\delta^{\mathcal{F}}$. Consider the path $\mathcal{P}_1 = \{A_q, A_{q-1}, \cdots, A_0 = (N, M)\}$ as a function $f(x)$ defined on the interval $[x_0, x_1]$ with $A_q = (x_0, f(x_0))$ and $A_0 = (x_1, f(x_1))$. By remark 4.3.4, we have the following inequalities: $slope(l_{A_0,A_1}) < \cdots < slope(l_{A_{q-1},A_q})$. This implies that the function f is concave. Therefore, for any two points in the domain of f, the function always lies on or above the line segment joining these two points. In particular, if we choose the points to be A_q and $A_0 = (N, M)$, we get that the points $A_q, A_{q-1}, ..., A_0 = (N, M)$ lie on or above the line segment l_1, implying that l_1 lies inside $M_\delta^{\mathcal{F}}$. The same argument can be repeated for the line segments l_2 and l_3. For the line segment l_4, a slight modification of the above argument works by considering the path $\mathcal{P}_4 = \{A_0 = (N, M), \cdots, B_u\}$ as a function $g(y)$ defined on the interval $[y_0, y_1]$ with $A_0 = (y_0, g(y_0))$ and $B_u = (y_1, g(y_1))$. □

Lemma 4.3.7. *Let $l_{N,M}^{a,b}$ and $l_{n,m}^{a,b}$ denote the line segments connecting the points (N, M) to (a, b) and (n, m) to (a, b) respectively, where $(a, b) \in S^{uc}$. Note from remark 4.2.7 that N, M, a, b depend on δ. Then*

- *Either $\lim_{\delta\to\infty} |slope(l_{N,M}^{a,b})| = 0$ for every $(a, b) \in S^{uc}$ or $\lim_{\delta\to\infty} |slope(l_{N,M}^{a,b})| = \infty$ for every $(a, b) \in S^{uc}$.*

- *Either $\lim_{\delta\to\infty} |slope(l_{n,m}^{a,b})| = 0$ or $\lim_{\delta\to\infty} |slope(l_{n,m}^{a,b})| = \infty$ or $\lim_{\delta\to\infty} |slope(l_{n,m}^{a,b})| = 1$ for $(a, b) \in S^{uc}$.*

Proof. Since $(a, b) \in S^{\text{uc}}, (N, M) \in S^{\text{uc}}$ and $(n, m) \in S^{\text{uc}}$, by remark 4.2.7, one can parametrize them as follows: $(N, M) = (e^{N'\delta}, e^{M'\delta}), (n, m) = (e^{n'\delta}, e^{m'\delta})$ and $(a, b) = (e^{a'\delta}, e^{b'\delta})$ for some $M', N', m', n', a', b' \in \mathbb{R}$. We aligned our analysis into the following cases:

Case I: Consider the line segment $l^{a,b}_{N,M}$, where $(a,b) \in S^{\text{uc}}$. Then, we have

$$|slope(l^{a,b}_{N,M})| = \left|\frac{e^{M'\delta} - e^{b'\delta}}{e^{N'\delta} - e^{a'\delta}}\right| \tag{4.3.8}$$

If in Step 2 of the construction of $M^{\mathcal{F}}_{\delta}$, M (or equivalently $e^{M'\delta}$) turns out to be the coordinate with the maximum value among points in S^{uc}, then we have

$$\lim_{\delta\to\infty} |slope(l^{a,b}_{N,M})| = \lim_{\delta\to\infty} \left|\frac{e^{M'\delta} - e^{b'\delta}}{e^{N'\delta} - e^{a'\delta}}\right| = \lim_{\delta\to\infty} \left|\frac{1 - e^{(b'-M')\delta}}{e^{(N'-M')\delta} - e^{(a'-M')\delta}}\right| = \infty \tag{4.3.9}$$

Else, if in Step 2 of the construction of $M^{\mathcal{F}}_{\delta}$, N (or equivalently $e^{N'\delta}$) turns out to be the coordinate with the maximum value among points in S^{uc}, then we have

$$\lim_{\delta\to\infty} |slope(l^{a,b}_{N,M})| = \lim_{\delta\to\infty} \left|\frac{e^{M'\delta} - e^{b'\delta}}{e^{N'\delta} - e^{a'\delta}}\right| = \lim_{\delta\to\infty} \left|\frac{e^{(M'-N')\delta} - e^{(b'-N')\delta}}{1 - e^{(a'-N')\delta}}\right| = 0. \tag{4.3.10}$$

Case II: Consider the line segment $l^{a,b}_{n,m}$, where $(a,b) \in S^{\text{uc}}$. Then, we have

$$|slope(l^{a,b}_{n,m})| = \left|\frac{e^{m'\delta} - e^{b'\delta}}{e^{n'\delta} - e^{a'\delta}}\right| \tag{4.3.11}$$

Let us assume that in Step 2 of the construction, we get $m = \min(\max(x_1, y_1), \max(x_2, y_2), ... , \max(x_p, y_p))$, where $(x_i, y_i) \in S^{\text{uc}}$. If $a' < b'$, we have $n' < m' < b'$ and

$$\lim_{\delta\to\infty} |slope(l^{a,b}_{n,m})| = \lim_{\delta\to\infty} \left|\frac{e^{m'\delta} - e^{b'\delta}}{e^{n'\delta} - e^{a'\delta}}\right| = \lim_{\delta\to\infty} \left|\frac{e^{(m'-b')\delta} - 1}{e^{(n'-b')\delta} - e^{(a'-b')\delta}}\right| = \infty. \tag{4.3.12}$$

Else if $a' > b'$, then we have $n' < m' < a'$ and

$$\lim_{\delta\to\infty} |slope(l^{a,b}_{n,m})| = \lim_{\delta\to\infty} \left|\frac{e^{m'\delta} - e^{b'\delta}}{e^{n'\delta} - e^{a'\delta}}\right| = \lim_{\delta\to\infty} \left|\frac{e^{(m'-a')\delta} - e^{(b'-a')\delta}}{e^{(n'-a')\delta} - 1}\right| = 0. \tag{4.3.13}$$

Else if $a' = b'$, then we have $n' < m' < a' = b'$ and

$$\lim_{\delta\to\infty} |slope(l^{a,b}_{n,m})| = \lim_{\delta\to\infty} \left|\frac{e^{m'\delta} - e^{a'\delta}}{e^{n'\delta} - e^{a'\delta}}\right| = \lim_{\delta\to\infty} \left|\frac{e^{(m'-a')\delta} - 1}{e^{(n'-a')\delta} - 1}\right| = 1. \tag{4.3.14}$$

If in Step 2 of the construction, we get $n = \min(\max(x_1, y_1), \max(x_2, y_2), ..., \max(x_p, y_p))$, a similar calculation shows that $\lim_{\delta\to\infty} |slope(l^{a,b}_{n,m})| = \infty$ when $a' > b'$, $\lim_{\delta\to\infty} |slope(l^{a,b}_{n,m})| = 0$ when $a' < b'$ and $\lim_{\delta\to\infty} |slope(l^{a,b}_{n,m})| = 1$ when $a' = b'$.

□

The next lemma shows that the cones C_{l_2,l_3} and C_{l_1,l_4} contain certain horizontal and vertical rays. Refer to Figure 4.7 for the proof of the next lemma.

Lemma 4.3.8. *For δ large enough, we have the following:*

- *The cone C_{l_2,l_3} contains the set $(n, m) + \mathbb{R}^2_{>0}$.*
- *The cone C_{l_1,l_4} either contains a fixed conical neighbourhood of the horizontal ray $(N, M) + \mathbb{R}_{<0} \times \{0\}$ or contains a fixed conical neighbourhood of the vertical ray $(N, M) + \{0\} \times \mathbb{R}_{<0}$ or contains both.*

Proof. We will first show that the cone C_{l_2,l_3} contains the set $(n, m) + \mathbb{R}^2_{>0}$. Note from remark 4.3.4 that we have the following set of inequalities: $slope(l_{C_r,C_{r-1}}) < \cdots < slope(l_{C_1,C_0}) < slope(l_{C_0,D_1}) < \cdots < slope(l_{D_{s-1},D_s}) < 0$. Let us denote the point $C_0 = (n, m)$ by (x_0, y_0). Let $C_1 = (x_1, y_1), C_2 = (x_2, y_2), ..., C_r = (x_r, y_r)$. Note that $y_0 - y_r = \sum_{i=1}^{r}(y_{i-1} - y_i) = \sum_{i=1}^{r} slope(l_{C_{i-1},i})(x_{i-1} - x_i)$. But we also have $y_0 - y_r = slope(l_2)(x_0 - x_r) = slope(l_2)\sum_{i=1}^{r}(x_{i-1} -$

x_i). This implies $slope(l_2) = \dfrac{\sum_{i=1}^{r} slope(l_{C_{i-1},i})(x_{i-1} - x_i)}{\sum_{i=1}^{r}(x_{i-1} - x_i)}$. Note that in the construction of $M_\delta^{\mathcal{F}}$, since we build line segments starting from (n, m) towards the point C_r by going along the attracting direction of the next uncertainty region in the clockwise sense, we have $x_i < x_{i-1}$ for $1 \leq i \leq r$. Therefore $slope(l_2)$ is a convex combination of the slopes of the line segments $l_{C_1,C_0}, l_{C_2,C_1}, ..., l_{C_{r-1},C_r}$ and is bounded by the maximum slope among these line segments. This implies that $slope(l_2) < slope(l_{C_1,C_0}) < 0$. A similar argument along the path $\{C_0, D_1, ..., D_s\}$ gives $slope(l_3) < slope(l_{D_{s-1},D_s}) < 0$. Consequently, the cone C_{l_2,l_3} contains the set $(n, m) + \mathbb{R}^2_{>0}$, as required.

We now show that the cone C_{l_1,l_4} either contains a fixed conical neighbourhood of the horizontal ray $(N, M) + \mathbb{R}_{<0} \times \{0\}$ or contains a fixed conical neighbourhood of the vertical ray $(N, M) + \{0\} \times \mathbb{R}_{<0}$ or contains both. In particular, we show that if in Step 2 of the construction of $M_\delta^{\mathcal{F}}$, M turns out to be the coordinate with the maximum value, then C_{l_1,l_4} contains a fixed conical neighbourhood of the vertical ray $(N, M) + \{0\} \times \mathbb{R}_{<0}$; and if N turns out to be the coordinate with the maximum value, then C_{l_1,l_4} contains a fixed conical neighbourhood of the horizontal ray $(N, M) + \mathbb{R}_{<0} \times \{0\}$. We present a proof for the case $M > N$, the other case follows analogously. Let us denote the coordinates of B_u by (x_u, y_u). By remark 4.3.2, we know that in the limit of large δ and for $M > N$, the path I_4 consists of an *almost* horizontal component and an *almost* vertical component separated by the line $Y = X$ in logarithmic space. Figure 4.8 depicts the path I_4 in logarithmic space. Note that from remark 4.2.7, one can parametrize $(N, M) = (e^{N'\delta}, e^{M'\delta})$ for some $M', N' \in \mathbb{R}$. By Lemma 4.3.3, we get that $x_u = c_1 M + c_2 = c_1 e^{M'\delta} + c_2$ for some $c_1, c_2 > 0$. Further, by

remark 4.3.1, we get that $y_u < 1$ and $M > 1$ or equivalently $M' > 0$. This gives

$$\begin{aligned}\lim_{\delta\to\infty} slope(l_4) &= \lim_{\delta\to\infty} \frac{y_u - M}{x_u - N} \\ &= \lim_{\delta\to\infty} \frac{y_u - e^{M'\delta}}{c_1 e^{M'\delta} + c_2 - e^{N'\delta}} \\ &= \lim_{\delta\to\infty} \frac{y_u/e^{M'\delta} - 1}{c_1 + c_2 e^{-M'\delta} - e^{(N'-M')\delta}} \\ &= \frac{-1}{c_1} < 0\end{aligned} \tag{4.3.15}$$

Let us denote the coordinates of A_q by (x_q, y_q). Note that in the construction of $M_\delta^{\mathcal{F}}$, since we build line segments starting from (N, M) towards the point A_q by going along the attracting direction corresponding to the next uncertainty region in an anticlockwise sense, we get $x_q < N$. This, together with Equation (4.3.15) implies that C_{l_1,l_4} contains a fixed conical neighbourhood of the vertical ray $(N, M) + \{0\} \times \mathbb{R}_{<0}$. □

The next lemma shows that for a sufficiently large δ, the set $\mathcal{M}_{\mathcal{F},\delta}$ contains all the intersection points corresponding to the uncertainty regions of the toric differential inclusion $\mathcal{T}_{\mathcal{F},\delta}$.

Lemma 4.3.9. *For large enough δ we have $S^{uc} \subset M_\delta^{\mathcal{F}}$.*

Proof. Refer to Figure 4.7 for this proof. Extend line segments l_1 and l_2 so that they meet at the point P_{12}. Let R_1 be the region enclosed between the curves C_{i_1}, C_{i_2} and the line segments joining A_0 to P_{12} and C_0 to P_{12}. Similarly, extend line segments l_3 and l_4 so that they meet at the point P_{34}. Let R_2 be the region formed between the curves C_{i_3}, C_{i_4} and the line segments joining A_0 to P_{34} and C_0 to P_{34}. Note that in the construction of $M_\delta^{\mathcal{F}}$, we stop building line segments at the uncertainty regions with indices i_1, i_2, i_3, i_4. Therefore, there is no element of S^{uc} in regions R_1 and R_2. By Lemma 4.3.8, we have that for δ large

enough, the cone C_{l_2,l_3} contains the set $(n,m)+\mathbb{R}^2_{>0}$ and the cone C_{l_1,l_4} either contains a fixed conical neighbourhood of the horizontal ray $(N,M)+\mathbb{R}_{<0}\times\{0\}$ or contains a fixed conical neighbourhood of the vertical ray $(N,M)+\{0\}\times\mathbb{R}_{<0}$ or contains both. By Lemma 4.3.7, for δ large enough, all the line segments connecting (N,M) to points in S^{uc} have either zero slope or all of them have infinite slope. This implies that all points in S^{uc} are contained in C_{l_1,l_4}. In addition, every line segment connecting (n,m) to points in S^{uc} has slope either zero, one or infinite, which implies that all points in S^{uc} are contained in C_{l_2,l_3}. Together, these arguments give us that $S^{\text{uc}}\in M_\delta^{\mathcal{F}}$ for δ large enough.

□

Lemma 4.3.10. *For large enough δ, we have $r(\boldsymbol{x})\leq 1$ for all $\boldsymbol{x}\in C_\delta^{\mathcal{F}}$.*

Proof. For contradiction, assume that there exists a $\boldsymbol{x}_0\in C_\delta^{\mathcal{F}}$ such that $r(\boldsymbol{x}_0)\geq 2$. Since $C_\delta^{\mathcal{F}}$ is a continuous curve, there exists a region D that is bounded by at least two different uncertainty regions such that it contains the point $\boldsymbol{x}_0$ in its interior. Further, steps 3 and 4 in the construction of $\mathcal{M}_{\mathcal{F},\delta}$ ensure that $C_\delta^{\mathcal{F}}$ intersects at least one uncertainty region containing $\boldsymbol{x}_0$ at both its boundary curves. This line segment of $C_\delta^{\mathcal{F}}$ containing $\boldsymbol{x}_0$ divides D into two regions. Therefore, there is at least element of S^{uc} that is not contained in $\mathcal{M}_{\mathcal{F},\delta}$, contradicting Lemma 4.3.9 which says that $S^{\text{uc}}\subseteq\mathcal{M}_{\mathcal{F},\delta}$ for a large enough δ. □

Proposition 4.3.11. *For large enough δ, $M_\delta^{\mathcal{F}}$ is an invariant region for the toric differential inclusion $\mathcal{T}_{\mathcal{F},\delta}$.*

Proof. Consider a solution $\boldsymbol{x}(t)$ of $\mathcal{T}_{\mathcal{F},\delta}$. We will show that if $\boldsymbol{x}(t_0)\in C_\delta^{\mathcal{F}}$, then $\dot{\boldsymbol{x}}(t_0)$ points towards the interior of $M_\delta^{\mathcal{F}}$ [3,18]. More precisely, we will show that $\dot{\boldsymbol{x}}(t_0)\cdot\boldsymbol{n}\leq 0$, where $\boldsymbol{n}$ is the outer normal to the curve $C_\delta^{\mathcal{F}}$. Note that by Lemma 4.3.10, we have that $r(\boldsymbol{x})\leq 1$ for all

$\boldsymbol{x} \in C_\delta^{\mathcal{F}}$. If $\boldsymbol{x} \in \mathcal{C}_{i_1} \cup \mathcal{C}_{i_2} \cup \mathcal{C}_{i_3} \cup \mathcal{C}_{i_4}$, then Lemma 4.3.5 shows that the cone corresponding to the right-hand side of $\mathcal{T}_{\mathcal{F},\delta}$ points towards the interior of the respective uncertainty regions. This implies that $\dot{\boldsymbol{x}}(t_0) \cdot \boldsymbol{n} \leq 0$. Else $\boldsymbol{x}$ lies on the line segments of $C_\delta^{\mathcal{F}}$. We proceed by case analysis:

Case 1: $r(\boldsymbol{x}(t_0)) = 1$. By remark 4.2.5.(i), the right-hand side of $\mathcal{T}_{\mathcal{F},\delta}$ is a half-space that points towards the interior of $M_\delta^{\mathcal{F}}$. Note that the slope of the generators of the half-space is equal to the slope of the line segment of $C_\delta^{\mathcal{F}}$ that contains the point $\boldsymbol{x}(t_0)$. Therefore, we have $\dot{\boldsymbol{x}}(t_0) \cdot \boldsymbol{n} \leq 0$.

Case 2: $r(\boldsymbol{x}(t_0)) = 0$. By remark 4.2.5.(iii), the right-hand side of $\mathcal{T}_{\mathcal{F},\delta}$ is a proper cone formed by the intersection of two half-spaces which are the right-hand sides of the toric differential inclusion corresponding to the nearest two uncertainty regions. Note that the half-space generated by the line segment of $C_\delta^{\mathcal{F}}$ that points towards $M_\delta^{\mathcal{F}}$ is one of these two half-spaces. By the analysis in Case 1, we get that the cone corresponding to the right-hand side of $\mathcal{T}_{\mathcal{F},\delta}$ is contained in both these half-spaces. In particular, it is contained in the half-space generated by the line segment of $C_\delta^{\mathcal{F}}$ that points towards $M_\delta^{\mathcal{F}}$. This implies that $\dot{\boldsymbol{x}}(t_0) \cdot \boldsymbol{n} \leq 0$.

□

Lemma 4.3.12. *For any $\delta > 0$ and $\boldsymbol{x}_0 \in \mathbb{R}^2_{>0}$, there exists a trajectory of $\mathcal{T}_{\mathcal{F},\delta}$ from $\boldsymbol{x}_0$ to $(1, 1)$.*

Proof. Using Proposition [5, 3.2], there exists a variable-k reversible dynamical system generated by $\mathcal{G} = (V, E)$ with

$$\epsilon = exp\left(\min_{\boldsymbol{s} \rightleftharpoons \boldsymbol{s}' \in E} ||\boldsymbol{s}' - \boldsymbol{s}|| \frac{\delta}{2}\right) \tag{4.3.16}$$

such that it can be embedded into the toric differential inclusion $\mathcal{T}_{\mathcal{F},\delta}$. Setting the rate constants $k_i = 1$ for all the reactions in $\mathcal{G}$, we get that $(1,1)$ is a point of complex balanced equilibrium. Since this dynamical system is two-dimensional, the point $(1,1)$ is a global attractor [9]. In particular, for any initial condition $\boldsymbol{x}(0) \in \mathbb{R}^2_{>0}$, a solution $\boldsymbol{x}(t)$ of this reversible dynamical system satisfies $\lim_{t\to\infty} \boldsymbol{x}(t) = (1,1)$. This implies that for any $\boldsymbol{x}_0 \in \mathbb{R}^2_{>0}$, there exists a trajectory of $\mathcal{T}_{\mathcal{F},\delta}$ from $\boldsymbol{x}_0$ to $(1,1)$. □

Corollary 4.3.13. *The point* $(1,1) \in \Omega^{min,inv}_{\mathcal{T}_{\mathcal{F},\delta}}$.

Proof. This follows from Lemma 4.3.12. □

Lemma 4.3.14. *For any* $\delta > 0$ *and* $\boldsymbol{x}_0 \in \mathbb{R}^2_{>0}$, *there exists a trajectory of* $\mathcal{T}_{\mathcal{F},\delta}$ *from* $\boldsymbol{x}_0$ *to* (N,M).

Proof. Note that from Step 2 in the construction of $M_{\mathcal{F},\delta}$, we have $(N,M) \in S^{\text{uc}}$. Without loss of generality, we can assume that (N,M) is the intersection of curves of the form $y^{q_i} = e^{\delta_i} x^{p_i}$ and $y^{q_j} = e^{\delta_j} x^{p_j}$. Consider the reaction network $\mathcal{G} = (V,E)$, where $E = \{q_iY \underset{k_2}{\overset{k_1}{\rightleftharpoons}} p_iX, q_jY \underset{k_4}{\overset{k_3}{\rightleftharpoons}} p_jX\}$. Using Proposition [5, 3.2], the variable-k reversible dynamical system generated by $\mathcal{G}$ with

$$\epsilon = exp\left(\min_{\boldsymbol{s}\rightleftharpoons\boldsymbol{s}'\in E} ||\boldsymbol{s}' - \boldsymbol{s}|| \frac{\delta}{2}\right) \tag{4.3.17}$$

can be embedded into the toric differential inclusion $\mathcal{T}_{\tilde{\mathcal{F}},\delta}$, where $\tilde{\mathcal{F}}$ is a fan whose line generators are given by $q_iY = p_iX$ and $q_jY = p_jX$. Setting the rate constants $k_1 = k_3 = 1, k_2 = e^{\delta_i}$ and $k_4 = e^{\delta_j}$ for this variable-k reversible dynamical system, we get that (N,M) is a point of complex balanced equilibrium. Since this dynamical system is two-dimensional, the point (N,M) is a global attractor [9]. In particular, for any initial condition $\boldsymbol{x}(0) \in \mathbb{R}^2_{>0}$,

a solution $\boldsymbol{x}(t)$ of this reversible dynamical system satisfies $\lim_{t\to\infty} \boldsymbol{x}(t) = (N, M)$. Note that since the line generators of $\tilde{\mathcal{F}}$ are included in the line generators of $\mathcal{F}$, by Lemma 4.2.2 we get that $\mathcal{T}_{\tilde{\mathcal{F}},\delta} \subseteq \mathcal{T}_{\mathcal{F},\delta}$. Therefore, this variable-k reversible dynamical system can be embedded into $\mathcal{T}_{\mathcal{F},\delta}$. This implies that for any $\boldsymbol{x}_0 \in \mathbb{R}^2_{>0}$, there exists a trajectory from $\boldsymbol{x}_0$ to (N, M). □

Lemma 4.3.15. *Consider the toric differential inclusion $\mathcal{T}_{\mathcal{F},\delta}$. Let UC_1, UC_2 be any two distinct uncertainty regions of $\mathcal{T}_{\mathcal{F},\delta}$. Then, we have $UC_1 \cap UC_2 \subseteq \Omega^{min,inv}_{\mathcal{F},\delta}$.*

Proof. For contradiction, assume that there exists $\boldsymbol{x}_0 \in \mathbb{R}^2_{>0}$ such that $\boldsymbol{x}_0 \in UC_1 \cap UC_2$ but $\boldsymbol{x}_0 \notin \Omega^{\mathrm{min,inv}}_{\mathcal{F},\delta}$. From remark 4.2.1, we know that $(1, 1)$ is in the interior of $UC_1 \cap UC_2$. From Corollary 4.3.13, we know that $(1, 1) \in \Omega^{\mathrm{min,inv}}_{\mathcal{F},\delta}$. Note that from remark 4.2.5.ii, we have $F_{\mathcal{F},\delta}(\boldsymbol{X}) = \mathbb{R}^2$ for all points $\boldsymbol{x} \in UC_1 \cap UC_2$. This implies that for any two points $\boldsymbol{x}_1, \boldsymbol{x}_2 \in UC_1 \cap UC_2$, there is a trajectory from $\boldsymbol{x}_1$ to $\boldsymbol{x}_2$. In particular, there exists a trajectory from $(1, 1)$ to $\boldsymbol{x}_0$, contradicting the fact that $\boldsymbol{x}_0 \notin \Omega^{\mathrm{min,inv}}_{\mathcal{F},\delta}$. □

Corollary 4.3.16. *The point $(1, 1)$ is contained in the interior of $\Omega^{min,inv}_{\mathcal{F},\delta}$.*

Proof. Follows from remark 4.2.1 and Lemma 4.3.15. □

Remark 4.3.17. Consider the points $\boldsymbol{x}_0, \boldsymbol{x}_1, \boldsymbol{x}_2 \in \mathbb{R}^2_{>0}$. Note that if there is a trajectory of $\mathcal{T}_{\mathcal{F},\delta}$ from $\boldsymbol{x}_0$ to $\boldsymbol{x}_1$ and from $\boldsymbol{x}_1$ to $\boldsymbol{x}_2$, then there exists a trajectory from $\boldsymbol{x}_0$ to $\boldsymbol{x}_2$. This follows from the fact that solutions of toric differential inclusions depend continuously on their initial conditions.

Lemma 4.3.18. *For any two points $\boldsymbol{x}_1$ and $\boldsymbol{x}_2$ in $\mathcal{M}_{\mathcal{F},\delta}$, there exists a trajectory from $\boldsymbol{x}_1$ to $\boldsymbol{x}_2$.*

Proof. We aligned our analysis into the following cases:

(i) $r(\boldsymbol{x}_2) \geq 2$: Note that from Lemma 4.3.12, we get that there is a trajectory from $\boldsymbol{x}_1$ to $(1,1)$. By remark 4.2.1, we know that the point $(1,1)$ is contained in every uncertainty region, implying that $r((1,1)) \geq 2$. Further, by remark 4.2.5.(ii), we know that $F_{\mathcal{F},\delta}(\boldsymbol{X}) = \mathbb{R}^2$ for every $\boldsymbol{x}$ such that $r(\boldsymbol{x}) \geq 2$. Therefore, there exists a trajectory from $(1,1)$ to the point $\boldsymbol{x}_2$. From remark 4.3.17, we get that there is a trajectory from $\boldsymbol{x}_1$ to $\boldsymbol{x}_2$, as desired.

(ii) $r(\boldsymbol{x}_2) = 1$: Let UC denote the uncertainty region that contains the point $\boldsymbol{x}_2$. From Lemma 4.3.14, we get that there is a trajectory from $\boldsymbol{x}_1$ to (N, M). Starting from (N, M), one can go along the boundary $C_\delta^{\mathcal{F}}$ till one reaches a point on the line segment intersecting the uncertainty region UC. Note that remark 4.2.5.(i) shows that the right-hand side of the toric differential inclusion at any point inside UC is a half-space that points towards the interior of $\mathcal{M}_{\mathcal{F},\delta}$. Therefore, there exists a trajectory from that point on the line segment intersecting UC to the point $\boldsymbol{x}_2$. From remark 4.3.17, we get that there that there is a trajectory from $\boldsymbol{x}_1$ to $\boldsymbol{x}_2$.

(iii) $r(\boldsymbol{x}_2) = 0$: Let UC_1 and UC_2 denote the two uncertainty regions closest to the point $\boldsymbol{x}_2$. From Lemma 4.3.14, we get that there is a trajectory from $\boldsymbol{x}_1$ to (N, M). Starting from (N, M), one can go along the curve $C_\delta^{\mathcal{F}}$ till one reaches a point P_1 on the boundary of the uncertainty region UC_1 that is closest to the point $\boldsymbol{x}_2$. From remark 4.2.5.(iii), the right-hand side of the toric differential inclusion at P_1 is a proper cone formed by the intersection of two half-spaces, which are the right-hand sides of the toric differential inclusion corrresponding to the uncertainty regions UC_1 and UC_2. Consider the region enclosed between the boundary of the uncertainty regions UC_1, UC_2 and $C_{\mathcal{F},\delta}$ such that $r(\boldsymbol{x}) = 0$ for every point $\boldsymbol{x}$ in this region. Note that the right-hand side of the toric differential inclusion at every point in this region is a

proper cone formed by the intersection of two half-spaces, which are the right-hand sides of the toric differential inclusion corrresponding to the uncertainty regions UC_1 and UC_2. In particular, this cone contains the point $\boldsymbol{x}_2$. Therefore, there exists a trajectory starting from the point P_1 to $\boldsymbol{x}_2$. From remark 4.3.17, we get that there is a trajectory from $\boldsymbol{x}_1$ to $\boldsymbol{x}_2$.

□

Finally we prove that the region $\mathcal{M}_{\mathcal{F},\delta}$ is the minimal invariant region.

Theorem 4.3.19. *For large enough δ, $\mathcal{M}_{\mathcal{F},\delta}$ is the minimal invariant region for the toric differential inclusion $\mathcal{T}_{\mathcal{F},\delta}$, i.e., $\mathcal{M}_{\mathcal{F},\delta} = \Omega^{min,inv}_{\mathcal{T}_{\mathcal{F},\delta}}$.*

Proof. By Lemma 4.3.11, we know that $\mathcal{M}_{\mathcal{F},\delta}$ is an invariant region for the toric differential inclusion $\mathcal{T}_{\mathcal{F},\delta}$. We now show that it is minimal, i.e., every invariant region contains $\mathcal{M}_{\mathcal{F},\delta}$. Note from the construction of $\mathcal{M}_{\mathcal{F},\delta}$ that the point (N, M) lies on the intersection of two uncertainty regions, i.e., $(N, M) \in S^{\text{uc}}$. By Lemma 4.3.15, the point (N, M) must belong to every invariant region. Further, by Lemma 4.3.18, there exists a trajectory from (N, M) to any point in $\mathcal{M}_{\mathcal{F},\delta}$. This implies that $\mathcal{M}_{\mathcal{F},\delta}$ is contained in every invariant region, as desired. □

Corollary 4.3.20. *The point $(1, 1)$ is contained in the interior of $\mathcal{M}_{\mathcal{F},\delta}$.*

Proof. Follows from Corollary 4.3.16 and thm 4.3.19. □

4.4 The minimal globally attracting region

The goal of this section is to show that $\mathcal{M}_{\mathcal{F},\delta}$ is the minimal globally attracting region for the toric differential inclusion $\mathcal{T}_{\mathcal{F},\delta}$. Towards this, we recall the construction of $\mathcal{M}_{\mathcal{F},\delta}$ from Section 4.2. Note that for δ large enough, the line segments connecting the polygonal paths I_1, I_2 and I_3, I_4 approach lines that are parallel to the coordinate axis, making the resultant polygon convex. Let $conv(\mathcal{M}_{\mathcal{F},\delta})$ denote the convex hull of $\mathcal{M}_{\mathcal{F},\delta}$. Therefore, for a sufficiently large δ, $conv(\mathcal{M}_{\mathcal{F},\delta})$ is a closed convex region enclosed by the polygon described above. Figure 4.11 shows $conv(\mathcal{M}_{\mathcal{F},\delta})$ for a sufficiently large δ.

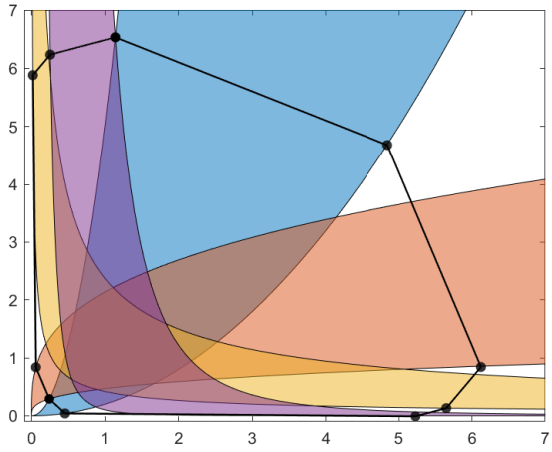

Figure 4.11: The $conv(\mathcal{M}_{\mathcal{F},\delta})$ for large δ.

Theorem 4.4.1. *Given a fan $\mathcal{F}$ and a sufficiently large δ, the region $\mathcal{M}_{\mathcal{F},\delta}$ is the minimal globally attracting region for the toric differential inclusion $\mathcal{T}_{\mathcal{F},\delta}$, i.e. $\Omega^{min,glob}_{\mathcal{T}_{\mathcal{F},\delta}} = \mathcal{M}_{\mathcal{F},\delta}$.*

Proof. We first show that $\mathcal{M}_{\mathcal{F},\delta} \subseteq \Omega^{\text{min,glob}}_{\mathcal{T}_{\mathcal{F},\delta}}$. Towards this, it is sufficient to show that every point in $\mathcal{M}_{\mathcal{F},\delta}$ is contained in the omega-limit set of some trajectory of $\mathcal{T}_{\mathcal{F},\delta}$. Note that by Lemma 4.3.12, there is a trajectory from $\boldsymbol{x}_0 \in \mathbb{R}^2_{>0}$ to the point $(1,1)$. In addition,

Corollary 4.3.20 shows that $(1,1)$ is in the interior of $\mathcal{M}_{\mathcal{F},\delta}$. Consider a point P in $\mathcal{M}_{\mathcal{F},\delta}$. By Lemma 4.3.18, we get that there is a trajectory from $(1,1)$ to P. Choose some $\zeta_1 > 0$. Then there is a trajectory $\boldsymbol{x}(t)$ of $\mathcal{T}_{\mathcal{F},\delta}$ with $\boldsymbol{x}(0) = (1,1)$, for which there exists $t_1 > 0$ such that $||\boldsymbol{x}(t_1) - P|| < \zeta_1$. Now choose some $\zeta_1' > 0$. By Lemma 4.3.12, there is a trajectory starting from $\boldsymbol{x}(t_1)$, for which there exists $t_1' > t_1$ such that $||\boldsymbol{x}(t_1') - (1,1)|| < \zeta_1'$. Now choose $0 < \zeta_2 < \zeta_1$. Again by Lemma 4.3.18, we get that there is a trajectory starting from $\boldsymbol{x}(t_1')$ for which there exists $t_2 > t_1' > t_1$ such that $||\boldsymbol{x}(t_2) - P|| < \zeta_2$. Repeating this back and forth between the points $(1,1)$ and P, we get a sequence of times $t_1 < t_2 < ... < t_k$ with $\lim_{k\to\infty} t_k = \infty$ such that $\lim_{k\to\infty} \boldsymbol{x}(t_k) = P$. This implies that the point P belongs to the omega-limit set of the trajectory $\boldsymbol{x}(t)$. Since the choice of the point P was arbitrary, the set $\mathcal{M}_{\mathcal{F},\delta}$ is contained in the minimal globally attracting region, i.e. $\mathcal{M}_{\mathcal{F},\delta} \subseteq \Omega^{\text{min,glob}}_{\mathcal{T}_{\mathcal{F},\delta}}$, as required.

We now show the other direction, i.e., $\Omega^{\text{min,glob}}_{\mathcal{T}_{\mathcal{F},\delta}} \subseteq \mathcal{M}_{\mathcal{F},\delta}$. Towards this, it suffices to show that $\mathcal{M}_{\mathcal{F},\delta}$ is a globally attracting region. Let us denote by $\mathcal{P}$ the boundary of $conv(\mathcal{M}_{\mathcal{F},\delta})$ and by $conv(\mathcal{P})$ the convex hull of $\mathcal{P}$. We will denote by $\mathcal{P}(\delta_0)$ the convex polygon corresponding to $\delta = \delta_0$ that can be constructed using the procedure described in Section 4.2 when δ_0 is large enough. Note that $\mathcal{P}(\delta)$ varies continuously with δ. In addition, we also have that $conv(\mathcal{P}(\delta))$ is a cover of $\mathbb{R}^2_{>0}$, i.e., $\bigcup_{\delta=\delta_0}^{\infty} conv(\mathcal{P}(\delta)) = \mathbb{R}^2_{>0}$ and $conv(\mathcal{P}(\delta')) \subset conv(\mathcal{P}(\delta''))$ if $\delta' < \delta''$. Now choose γ small enough so that $M^{\mathcal{F}}_{\delta_0-\gamma}$ can still be constructed. Consider a strict solution $\boldsymbol{x}(t)$ of the toric differential inclusion $\mathcal{T}^{\mathcal{F}}_{\delta}$ with initial condition $\boldsymbol{x}(0) \in \mathbb{R}^2_{>0}$. We will show that $\boldsymbol{x}(t) \in conv(\mathcal{P}(\delta_0))$ for a sufficiently large t.

Note that since we have $\bigcup_{\delta=\delta_0-\gamma}^{\infty} conv(\mathcal{P}(\delta)) = \mathbb{R}^2_{>0}$, one can choose $\delta_1 > \delta_0$ such that

$\boldsymbol{x}(0) \in \bigcup_{\delta=\delta_0-\gamma}^{\delta_1} conv(\mathcal{P}(\delta))$. Define a function $\Phi : \bigcup_{\delta=\delta_0-\gamma}^{\delta_1} \mathcal{P}(\delta) \to [\delta_0 - \gamma, \delta_1]$ such that

$$\Phi(x, y) = \delta \text{ if } (x, y) \in \mathcal{P}(\delta). \tag{4.4.1}$$

We will show that $\Phi(\boldsymbol{x}(t)) \leq \delta_0$ for t large enough. For contradiction, assume not. Then since $\Phi^{-1}[0, \delta_0] = conv(\mathcal{P}(\delta_0))$ and $\Phi^{-1}[0, \delta_1] = conv(\mathcal{P}(\delta_1))$ are invariant by Lemma 4.3.11, we get $\Phi(\boldsymbol{x}(t)) \in (\delta_0, \delta_1]$ for all t.

The function Φ is differentiable on its domain except at the points in the following set $\mathcal{W} = \{B_u, B_{u-1}, B_p, B_{p-1}, \cdots, B_1, A_0 = (N, M), A_1, A_2, \cdots, A_q, C_r, C_{r-1} \cdots, C_1, C_0 = (n, m), D_1, D_2, \cdots, D_s\}$. Consider $\boldsymbol{x}_0 \in \mathcal{W}$. Let Φ_1 and Φ_2 denote the smooth functions that define Φ on the two line segments in a neighborhood of $\boldsymbol{x}_0$. The subgradient of Φ at $\boldsymbol{x}_0$ is [20, Definition 8.3]

$$\partial\Phi(\boldsymbol{x}_0) = \{\lambda \boldsymbol{\nabla}\Phi_1(\boldsymbol{x}_0) + (1 - \lambda)\boldsymbol{\nabla}\Phi_2(\boldsymbol{x}_0) \mid \lambda \in [0, 1]\} \tag{4.4.2}$$

This subgradient $\partial\Phi$ exists and is continuous [20, Definition 9.1]. One can compose Φ with $\boldsymbol{x}(t)$ which is differentiable to get a strictly continuous function $\Phi \circ \boldsymbol{x}(t)$. Consequently, one can apply a generalized mean value thm [20, thm 10.48] to $\Phi \circ \boldsymbol{x}(t)$ to get that there exists a $t_0 \in [0, t]$ such that

$$\Phi(\boldsymbol{x}(t)) - \Phi(\boldsymbol{x}(0)) = t g_t \text{ for some } g_t \in \partial(\Phi \circ \boldsymbol{x})(t_0) \tag{4.4.3}$$

By the chain rule [20, thm 10.6], we have

$$\partial(\Phi \circ \boldsymbol{x})(t) \subset \{\boldsymbol{w} \cdot \dot{\boldsymbol{x}}(t) \,|\, \boldsymbol{w} \in \partial\Phi(\boldsymbol{x}(t))\}. \tag{4.4.4}$$

Note that Lemma 4.3.11 proves that $\mathcal{M}_{\mathcal{F},\delta}$ is invariant by showing that along its boundary,

the vector field points towards the interior of $\mathcal{M}_{\mathcal{F},\delta}$. In particular, we can extend this proof to show that for a compact set $J \in \mathbb{R}^2_{>0}$, there exists a $\eta > 0$ such that for $\boldsymbol{x}(t) \in J$, we have $\boldsymbol{\nabla}\Phi_1(\boldsymbol{x}(t)) \cdot \dot{\boldsymbol{x}}(t) < -\eta$ and $\boldsymbol{\nabla}\Phi_2(\boldsymbol{x}(t)) \cdot \dot{\boldsymbol{x}}(t) < -\eta$. Note that from Equation (4.4.2), we have that the subgradient $\partial\Phi(\cdot)$ is a convex combination of $\boldsymbol{\nabla}\Phi_1(\cdot)$ and $\boldsymbol{\nabla}\Phi_2(\cdot)$. This implies that $\partial\Phi(\boldsymbol{x}(t))\dot{\boldsymbol{x}}(t) < -\eta$. Using Equation (4.4.4), we get

$$\sup_{t\geq 0} \partial(\Phi \circ \boldsymbol{x})(t) < -\eta \tag{4.4.5}$$

From the mean value thm given by Equation (4.4.3), we get

$$\Phi(\boldsymbol{x}(t)) < \Phi(\boldsymbol{x}(0)) - \eta t \tag{4.4.6}$$

for all $t > 0$, contradicting that $\Phi(\boldsymbol{x}(t)) \in [\delta_0, \delta_1]$ for all $t \geq 0$.

Therefore, $\boldsymbol{x}(t) \in conv(\mathcal{P}(\delta_0)) = conv(M^{\mathcal{F}}_{\delta_0})$ for t large enough. If $\boldsymbol{x}(t) \in conv(M^{\mathcal{F}}_{\delta_0}) \setminus M^{\mathcal{F}}_{\delta_0}$, then our construction of $M^{\mathcal{F}}_{\delta_0}$ would imply $r(\boldsymbol{x}) = 0$. Since $\boldsymbol{x}(t)$ is a strict solution, we would have $\boldsymbol{x}(t_0) \in \mathcal{C}_{i_1} \cup \mathcal{C}_{i_2} \cup \mathcal{C}_{i_3} \cup \mathcal{C}_{i_4} \in M^{\mathcal{F}}_{\delta_0}$ for t_0 large enough. This implies that $M^{\mathcal{F}}_{\delta_0}$ is a globally attracting region, as desired. □

4.5 Special cases

Note that the construction of $\mathcal{M}_{\mathcal{F},\delta}$ outlined in Section 4.2 makes certain assumptions on the underlying fan; in particular see Assumption 4.2.6. In this section, we show how to handle the cases when (i) the line generators of the fan have either all positive slopes or all negative slopes or (ii) at least one line generator of the fan has zero slope or infinite slope. In both these cases, the construction of $\mathcal{M}_{\mathcal{F},\delta}$ proceeds like in Section 4.2, albeit with certain modifications as we show below.

- *If the line generators of the fan have either all positive slopes or all negative slopes*: The procedure for the case with all positive slopes is completely analogous with the procedure outlined in Section 4.2. We present a procedure for the case with all negative slopes. The starting point (N, M) is chosen as described in Step 2 of Section 4.2. The starting point (n, m) is chosen differently as shown in Figure 4.12. The construction of $\mathcal{M}_{\mathcal{F},\delta}$ then proceeds like in Section 4.2.

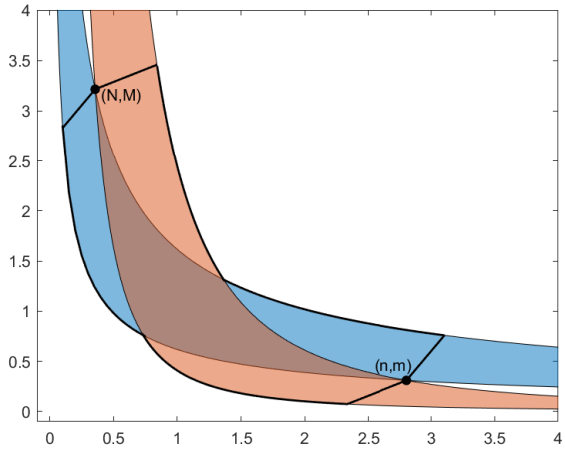

Figure 4.12: The construction of $\mathcal{M}_{\mathcal{F},\delta}$ when the line generators of the fan have all negative slopes.

- *If at least one line generator of the fan has zero or infinite slope*: For example, if one of the line generators of the fan has zero slope, then the construction proceeds exactly as described in Section 4.2 until Step 4. In Step 5, we complete the boundary of $\mathcal{M}_{\mathcal{F},\delta}$ by a vertical line segment joining the polygonal paths I_1 and I_2 as shown in Figure 4.13. Note that it is possible that the construction of $\mathcal{M}_{\mathcal{F},\delta}$ might make either the point (N, M) or (n, m) an interior point of $\mathcal{M}_{\mathcal{F},\delta}$.

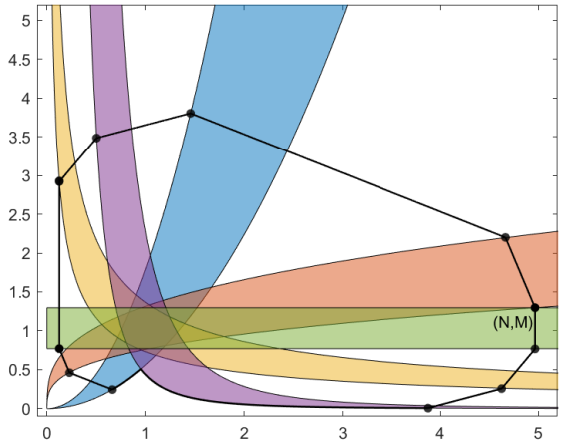

Figure 4.13: The construction of $\mathcal{M}_{\mathcal{F},\delta}$ when a line generator of the fan has zero slope.

4.6 Discussion

We have shown how to construct the minimal invariant region for a toric differential inclusion. Additionally, we have shown that the minimal invariant region is also the minimal globally attracting region for the toric differential inclusion. These results are very relevant in the study of mass-action systems and more generally polynomial dynamical systems, since it is known that weakly reversible and endotactic dynamical systems can be embedded into toric differential inclusions [5, 6], which is a key step towards the proposed proof of the global attractor conjecture [4]. It is notable that the structure of toric differential inclusions gives their solutions a greater degree of freedom as compared to the solutions of variable-k mass-action systems. The minimal invariant regions constructed in this paper are also invariant regions for appropriate variable-k mass-action systems. Further, the minimal globally attracting regions allow us to give *uniform upper and lower bounds* on the solutions of variable-k mass action systems when $t \to \infty$.

On the other hand, solutions of variable-k mass-action systems are confined to a

proper subset of the right-hand side of the corresponding toric differential inclusion, since the rate constants of the reactions cannot be switched off completely. It would be interesting to explore how to build minimal invariant and minimal globally attracting regions for variable-k mass-action systems, which we plan to do in upcoming work.

Chapter 5

Minimal invariant and minimal globally attracting regions for variable-k dynamical systems

5.1 Introduction

In this chapter, we bring up the questions of how to find the minimal invariant regions and the minimal globally attracting regions in the variable-k dynamical systems. In section 5.2, we divide general variable-k dynamical systems with two reactions into 6 different cases according to the slopes of their line generators; in section 5.3 and 5.4 we construct the minimal invariant regions and the minimal globally attracting regions in variable-k dynamical systems for all six cases, we also give a prove for those cases; in 5.5 we discuss some example of variable-k dynamical systems with three reactions; we analyse the difficulties and give a conjecture of a possible way to construct the minimal invariant region and the minimal globally attracting regions for the variable-k dynamical systems with three reactions.

5.2 Variable-k dynamical systems with two reactions

Consider the following reaction network:

$$\begin{aligned} a_1X + b_1Y &\underset{k_2(t)}{\overset{k_1(t)}{\rightleftharpoons}} a_1'X + b_1'Y \\ a_2X + b_2Y &\underset{k_4(t)}{\overset{k_3(t)}{\rightleftharpoons}} a_2'X + b_2'Y \end{aligned} \tag{5.2.1}$$

where $a_1, a_1', a_2, a_2' \in \mathbb{R}_{\geq 0}$ and $\epsilon \leq k_1(t), k_2(t) \leq \frac{1}{\epsilon}$.

We will consider the case when $(a_1' - a_1) \cdot (b_1' - b_1) < 0$, $\frac{a_1 - a_1'}{b_1' - b_1} > 1$ and $(a_2' - a_2) \cdot (b_2' - b_2) < 0$, $\frac{a_2 - a_2'}{b_2' - b_2} < 1$; the analysis for other cases will proceed analogously. Consider the four equilibrium curves:

- $\mathcal{C}_1 : x^{a_1' - a_1} y^{b_1' - b_1} = \epsilon^2$
- $\mathcal{C}_2 : x^{a_1' - a_1} y^{b_1' - b_1} = \frac{1}{\epsilon^2}$.
- $\mathcal{C}_3 : x^{a_2' - a_2} y^{b_2' - b_2} = \epsilon^2$
- $\mathcal{C}_4 : x^{a_2' - a_2} y^{b_2' - b_2} = \frac{1}{\epsilon^2}$.

The points (A, B, C, D) are given by the intersection of these curves.

According to the parameters we choose, there are three different kind of curves. Therefore for two reactions, the combinations give six different cases:

- $(a_1' - a_1) \cdot (b_1' - b_1) < 0$, $\frac{a_1 - a_1'}{b_1' - b_1} > 1$ and $(a_2' - a_2) \cdot (b_2' - b_2) < 0$, $\frac{a_2 - a_2'}{b_2' - b_2} < 1$.
- $(a_1' - a_1) \cdot (b_1' - b_1) < 0$, $\frac{a_1 - a_1'}{b_1' - b_1} > 1$ and $(a_2' - a_2) \cdot (b_2' - b_2) < 0$, $\frac{a_2 - a_2'}{b_2' - b_2} > 1$.

- $(a_1' - a_1) \cdot (b_1' - b_1) < 0$, $\frac{a_1 - a_1'}{b_1' - b_1} < 1$ and $(a_2' - a_2) \cdot (b_2' - b_2) < 0$, $\frac{a_2 - a_2'}{b_2' - b_2} < 1$.
- $(a_1' - a_1) \cdot (b_1' - b_1) > 0$, $\frac{a_1 - a_1'}{b_1' - b_1} < 0$ and $(a_2' - a_2) \cdot (b_2' - b_2) > 0$, $\frac{a_2 - a_2'}{b_2' - b_2} < 0$.
- $(a_1' - a_1) \cdot (b_1' - b_1) < 0$, $\frac{a_1 - a_1'}{b_1' - b_1} > 1$ and $(a_2' - a_2) \cdot (b_2' - b_2) > 0$, $\frac{a_2 - a_2'}{b_2' - b_2} < 0$.
- $(a_1' - a_1) \cdot (b_1' - b_1) < 0$, $\frac{a_1 - a_1'}{b_1' - b_1} < 1$ and $(a_2' - a_2) \cdot (b_2' - b_2) > 0$, $\frac{a_2 - a_2'}{b_2' - b_2} < 0$.

We will analyze each case and give a construction of the minimal invariant region and the minimal globally attracting region for all different cases.

5.3 Minimal invariant region and minimal globally attracting region of two reaction with same directions

In this section we discuss what happens in case $1-4$, in which the two reactions have the same directions for their line generators.

Lemma 5.3.1. *If two reactions are in the same direction, the trajectories start from the vertexes end in the neighboring vertexes won't travel across the curve. For example, the trajectory $traj(AB)$ will not cross that curve AB.*

Proof. The trajectory starts at point A, it must start in one side of the curve AB. We will prove that it will stay the same side it starts.

Assume the trajectory from A to B does not stay on the same side of curve AB, then there must exist a point P on curve AB, such that the trajectory will intersect with curve AB at the point P and then the trajectory will go to the other side. However, since the

point P is on the curve AB, at the P one of the specific reaction(corresponding to AB) is balanced, so the differential equation will be given by the other reaction, which would give a direction vector in the same direction as at point A. Therefore, rather than cross to the other side, the trajectory will stay on the same side as start. □

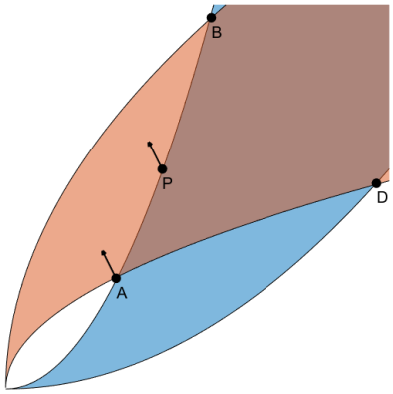

Figure 5.1: All trajectories in OAB which go to B won't cross the curve AB

Proposition 5.3.2. *In variable-k system, for any two points P, Q, if there is a curve connecting P, Q, and for a trajectory goes from P to Q, the direction vector on the curve always stay on one side of the curve, then the trajectory will not go across the curve.*

Proof. Assume the trajectory go across the curve at some point M, then at point P and M the direction vectors are not on the same side, this leads to a contradiction. □

Proposition 5.3.3 (The region $\mathcal{M}_\epsilon$)**.** *There are four vertexes with fixed cones of angle θ or $\pi - \theta$(with $\frac{\pi}{2} < \theta < \pi$). Then choose the two points with the angle θ as starting points, the other two as the end points, we can form four trajectories by solving the differential equations. We denote this region $\mathcal{M}_\epsilon$.*

Now we are going to prove that the closed region bounded by these special trajectories is the minimal invariant region.

Proposition 5.3.4. *In cases* $1, 2, 3, 4$*, the region* $\mathcal{M}_\epsilon$ *stays inside the uncertainty regions.*

Proof. We now prove the case 1, the other cases can be proved with the same idea.

In this case, the trajectories start from the points A, C. go to the points B, D. By lemma 5.3.1 the trajectory won't cross the curve AB. We want to prove that the trajectory will be bounded in the closed region with three vertexes O(the origin), A and B. If the trajectories travel to the upper bound which goes through O, B and to the left of the point B, the reaction which goes through the point O, B will be balanced and the the attracting direction will be given by the reaction goes through A, B, in the direction $-\frac{a_2-a_2'}{b_2'-b_2}$, which points to the fourth quadrant, so it won't leave the upper left bound of the uncertainty region. In the interior of this region, the attracting direction will be bounded by $-\frac{a_1-a_1'}{b_1'-b_1}$ and $-\frac{a_2-a_2'}{b_2'-b_2}$, which does not contain the third quadrant, so the trajectory start from the point A will never travel to the part of the curve bounded by O and A. Similarly, we can prove it also stay in the other uncertainty regions.

□

Definition 5.3.5 (Reaction curves)**.** Consider a dynamical system $\mathcal{G}_\epsilon^{\text{variable-k}}$ with two reactions, the curve $\mathcal{C}_\infty$ is defined as

$$y^{q_1} = \epsilon^2 x^{p_1}, \quad \text{while } q_1 = |b_1 - b_1'|,\ p_1 = |a_1 - a_1'|. \tag{5.3.1}$$

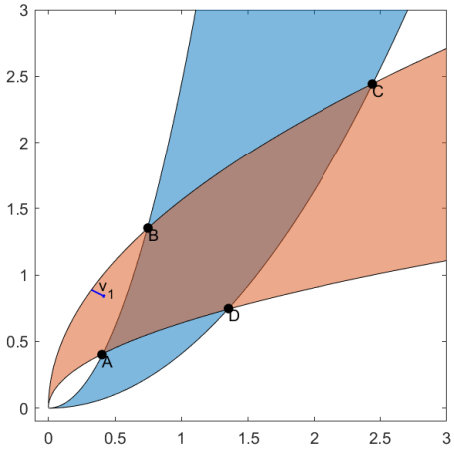

Figure 5.2: All trajectories in OAB which go to B won't cross the curve OB

Definition 5.3.6 (Closed regions)**.** Consider a dynamical system $\mathcal{G}_\epsilon^{\text{variable-k}}$ with two reactions, and A, B, C, D be the different intersection points of the boundary of each reactions. Then $R(AB)$ will be the closed region bounded by curve $\mathcal{C}_3$, $\mathcal{C}_4$ and AB; similarly we can define it for $R(BC)$, $R(CD)$ and $R(DA)$. And the region $R(ABCD)$ be the closed region boundary by the curve $\mathcal{C}_1$, $\mathcal{C}_2$, $\mathcal{C}_3$ and $\mathcal{C}_4$.

Proposition 5.3.7. *In cases* $1, 2, 3, 4$, $\mathcal{M}_\epsilon$ *is an invariant region for* $\mathcal{G}_\epsilon^{\text{variable-k}}$.

Proof. Now we prove with an example,

$$\begin{aligned} a_1X + b_1Y &\underset{k_1(t)}{\overset{k_2(t)}{\rightleftharpoons}} a_1'X + b_1'Y \\ a_2X + b_2Y &\underset{k_3(t)}{\overset{k_4(t)}{\rightleftharpoons}} a_2'X + b_2'Y \end{aligned} \tag{5.3.2}$$

while $a_1 - a_1' > b_1' - b_1 > 0$ and $b_2' - b_2 > a_2 - a_2' > 0$. This proof also works for any other variable-k system with 2 species.

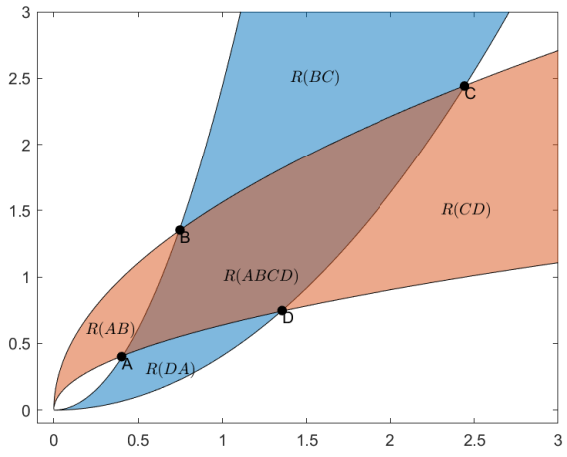

Figure 5.3

Since the variable-k system can be embedded into the toric differential inclusion $\mathcal{T}_{\mathcal{F},\delta}.0$ We know that when ϵ is small enough all the trajectory should stay in 5 regions shown in figure 5.3.

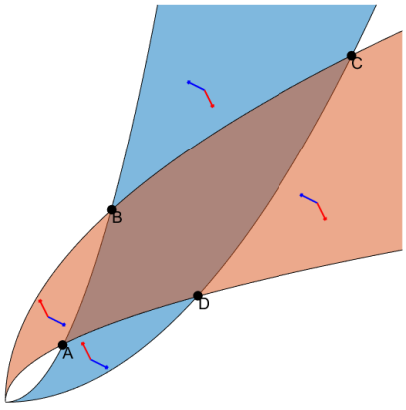

Figure 5.4

The whole region $R(ABCD)$ should be included in the minimal invariant region since

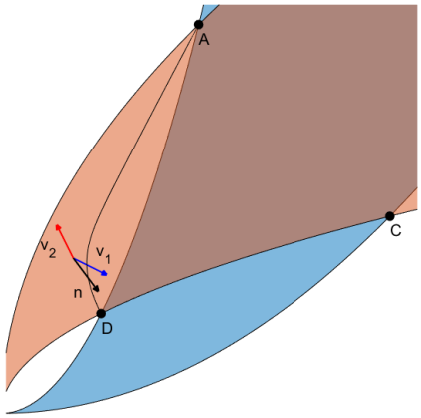

Figure 5.5

any point in region $R(ABCD)$ can be a equilibrium point when choose some proper values of $k_i \in [\epsilon, \frac{1}{\epsilon}]$.

In region $R(AB)$, any trajectory start and end in this closed region will be bounded within the region, we will show that these trajectories cannot cross the boundary of the region, the system will be governed by the reactions as follow

$$\begin{aligned} a_1X + b_1Y &\underset{\epsilon}{\overset{\frac{1}{\epsilon}}{\rightleftharpoons}} a_1'X + b_1'Y \\ a_2X + b_2Y &\underset{\epsilon}{\overset{\frac{1}{\epsilon}}{\rightleftharpoons}} a_2'X + b_2'Y \end{aligned} \tag{5.3.3}$$

And we denote

$$\boldsymbol{v}_1 = \begin{pmatrix} a_1 - a_1' \\ b_1 - b_1' \end{pmatrix} \tag{5.3.4}$$

$$\boldsymbol{v}_2 = \begin{pmatrix} a_2' - a_2 \\ b_2' - b_2 \end{pmatrix} \tag{5.3.5}$$

Then

$$\boldsymbol{v}_1 \cdot \mathbf{n} > 0 \tag{5.3.6}$$

$$\boldsymbol{v}_2 \cdot \mathbf{n} \leq 0 \tag{5.3.7}$$

The trajectory $traj(AB)$ from A to B is given by the following system of ODE.

$$\begin{pmatrix} \dot{x} \\ \dot{y} \end{pmatrix} = \left(\epsilon x^{a_1} y^{b_1} - \frac{1}{\epsilon} x^{a_1'} y^{b_1'}\right)\boldsymbol{v}_1 - \left(\epsilon x^{a_2} y^{b_2} - \frac{1}{\epsilon} x^{a_2'} y^{b_2'}\right)\boldsymbol{v}_2 \tag{5.3.8}$$

Let $\mathbf{n}$ denote the inward pointing normal to the trajectory given by Equation 5.3.8. Then we get

$$\left[\begin{pmatrix} \dot{x} \\ \dot{y} \end{pmatrix} = \left(\epsilon x^{a_1} y^{b_1} - \frac{1}{\epsilon} x^{a_1'} y^{b_1'}\right)\boldsymbol{v}_1 - \left(\epsilon x^{a_2} y^{b_2} - \frac{1}{\epsilon} x^{a_2'} y^{b_2'}\right)\boldsymbol{v}_2 \right] \cdot \mathbf{n} = 0 \tag{5.3.9}$$

Note that by construction, we have

$$\boldsymbol{v}_1 \cdot \mathbf{n} > 0 \tag{5.3.10}$$

$$\boldsymbol{v}_2 \cdot \mathbf{n} \leq 0 \tag{5.3.11}$$

. Since $\epsilon \leq k_1(t), k_2(t), k_3(t), k_4(t) \leq \frac{1}{\epsilon}$, we get the following

$$\left(k_2(t)x^{a_1}y^{b_1} - k_1(t)x^{a_1'}y^{b_1'}\right)\boldsymbol{v}_1 \cdot \mathbf{n} \geq \left(\epsilon x^{a_1}y^{b_1} - \frac{1}{\epsilon}x^{a_1'}y^{b_1'}\right)\boldsymbol{v}_1 \cdot \mathbf{n} \tag{5.3.12}$$

and

$$\left(k_4(t)x^{a_2}y^{b_2} - k_3(t)x^{a_2'}y^{b_2'}\right)\boldsymbol{v}_2 \cdot \mathbf{n} \leq \left(\frac{1}{\epsilon}x^{a_2}y^{b_2} - \epsilon x^{a_2'}y^{b_2'}\right)\boldsymbol{v}_2 \cdot \mathbf{n} \tag{5.3.13}$$

Adding Equations 5.3.12 and 5.3.13 and using Equation 5.3.9, we get that

$$\left[\left(k_2(t)x^{a_1}y^{b_1} - k_1(t)x^{a_1'}y^{b_1'}\right)\boldsymbol{v}_1 - \left(k_4(t)x^{a_2}y^{b_2} - k_3(t)x^{a_2'}y^{b_2'}\right)\boldsymbol{v}_2\right] \cdot \mathbf{n} \geq 0 \tag{5.3.14}$$

as required.

Similarly in region $R(BC)$, $R(CD)$, $R(DA)$, we can repeat the same proof. Therefore, when ϵ is small enough, $\mathcal{M}_\epsilon$ is an invariant region for $\mathcal{G}_\epsilon^{\text{variable-k}}$. □

Proposition 5.3.8. *Consider a dynamical system $\mathcal{G}_\epsilon^{\text{variable-k}}$. Then $\mathcal{M}_\epsilon$ is an invariant region for $\mathcal{G}_\epsilon^{\text{variable-k}}$.*

Proof. The trajectory between C and D is given by the following system of ODE.

$$\begin{pmatrix}\dot{x}\\ \dot{y}\end{pmatrix} = \left(\epsilon x^{a_1}y^{b_1} - \frac{1}{\epsilon}x^{a_1'}y^{b_1'}\right)\begin{pmatrix}a_1 - a_1'\\ b_1 - b_1'\end{pmatrix} + \left(\frac{1}{\epsilon}x^{a_2}y^{b_2} - \epsilon x^{a_2'}y^{b_2'}\right)\begin{pmatrix}a_2 - a_2'\\ b_2 - b_2'\end{pmatrix}$$

Let $\mathbf{n}$ denote the inward pointing normal to the trajectory given by Equation 5.3.8. Then we get

$$\left[\begin{pmatrix}\dot{x}\\ \dot{y}\end{pmatrix} = \left(\epsilon x^{a_1}y^{b_1} - \frac{1}{\epsilon}x^{a_1'}y^{b_1'}\right)\begin{pmatrix}a_1 - a_1'\\ b_1 - b_1'\end{pmatrix} + \left(\frac{1}{\epsilon}x^{a_2}y^{b_2} - \epsilon x^{a_2'}y^{b_2'}\right)\begin{pmatrix}a_2 - a_2'\\ b_2 - b_2'\end{pmatrix}\right] \cdot \mathbf{n} = 0$$

Note that by construction, we have $\begin{pmatrix}a_1 - a_1'\\ b_1 - b_1'\end{pmatrix} \cdot \mathbf{n} > 0$ and $\begin{pmatrix}a_2 - a_2'\\ b_2 - b_2'\end{pmatrix} \cdot \mathbf{n} \leq 0$. Since $\epsilon \leq k_1(t), k_2(t), k_3(t), k_4(t) \leq \frac{1}{\epsilon}$, we get the following

$$\left(k_2(t)x^{a_1}y^{b_1} - k_1(t)x^{a_1'}y^{b_1'}\right)\begin{pmatrix}a_1 - a_1'\\ b_1 - b_1'\end{pmatrix} \cdot \mathbf{n} \geq \left(\epsilon x^{a_1}y^{b_1} - \frac{1}{\epsilon}x^{a_1'}y^{b_1'}\right)\begin{pmatrix}a_1 - a_1'\\ b_1 - b_1'\end{pmatrix} \cdot \mathbf{n}$$

and

$$\left(k_4(t)x^{a_2}y^{b_2} - k_3(t)x^{a_2'}y^{b_2'}\right)\begin{pmatrix}a_2 - a_2'\\ b_2 - b_2'\end{pmatrix} \cdot \mathbf{n} \geq \left(\frac{1}{\epsilon}x^{a_2}y^{b_2} - \epsilon x^{a_2'}y^{b_2'}\right)\begin{pmatrix}a_2 - a_2'\\ b_2 - b_2'\end{pmatrix} \cdot \mathbf{n}$$

Adding Equations 5.3.12 and 5.3.13 and using Equation 5.3.9, we get that

$$\left[\left(k_2(t)x^{a_1}y^{b_1} - k_1(t)x^{a_1'}y^{b_1'}\right)\begin{pmatrix} a_1 - a_1' \\ b_1 - b_1' \end{pmatrix} + \left(k_4(t)x^{a_2}y^{b_2} - k_3(t)x^{a_2'}y^{b_2'}\right)\begin{pmatrix} a_2 - a_2' \\ b_2 - b_2' \end{pmatrix}\right] \cdot \mathbf{n} \geq 0$$

as required.

□

Lemma 5.3.9. *Consider a dynamical system $\mathcal{G}_\epsilon^{\text{variable-k}}$. Let P_1 and P_2 be points in $\mathcal{M}_\epsilon$. Then $P_1 \rightsquigarrow_{\text{variable-k}} P_2$.*

Proof. Any point (x, y) in region $\mathcal{K}$ is the intersection of two equilibrium curves $k_2 x^{a_1} y^{b_1} = k_1 x^{a_1'} y^{b_1'}$ and $k_4 x^{a_2} y^{b_2} = k_3 x^{a_2'} y^{b_2'}$ for some rate constants $\epsilon \leq k_1, k_2, k_3, k_4 \leq \frac{1}{\epsilon}$. Therefore, the point (x, y) is detailed balanced for these values of rate constants. Since $\mathcal{G}$ is a two dimensional reversible E-graph, the point (x, y) is a global attractor for these values of rate constants. In particular, this implies that if for every $\delta > 0$ and any solution $(x(t), y(t))$ of this dynamical system with $(x(0), y(0)) \in \mathbb{R}^2_{>0}$, there exists $T > 0$ such that for all $t > T$, we have $(x(t), y(t)) \in \mathcal{N}_\delta(x, y)$.

Consider a point (x, y) in $\mathcal{M} \setminus \mathcal{K}$. Draw a line corresponding to the attracting directions of the uncertainty region in which it is not a part of and see where it intersects the curve. Call this point F. Run the same trajectory starting from C until you reach the point F. Now choose rate constants so that it corresponds to the equilibrium curve of the point F. Run the trajectory with these rate constants till you reach the point P. □

Proposition 5.3.10. *Consider a dynamical system $\mathcal{G}_\epsilon^{\text{variable-k}}$. Then $\mathcal{M}_\epsilon$ is a globally attracting region for $\mathcal{G}_\epsilon^{\text{variable-k}}$.*

Proof. Let ϵ_0 be small enough so that the region $\mathcal{M}_{\epsilon_0}$ can be constructed according to the procedure described in Section 2. Note that $\mathcal{M}_\epsilon$ varies continuously as a function of ϵ. In addition, we have $\bigcup_{\epsilon\in(0,\epsilon_0]} \mathcal{M}_\epsilon = \mathbb{R}^2_{>0}$. Let ζ be small enough so that the region $\mathcal{M}_{\epsilon_0+\zeta}$ can still be constructed. Let $\boldsymbol{x}(t)$ be a solution of $\mathcal{G}_\epsilon^{\text{variable-k}}$ with $\boldsymbol{x}(0) \in \mathbb{R}^2_{>0}$. Since $\bigcup_{\epsilon\in(0,\epsilon_0+\zeta]} \mathcal{M}_{\epsilon+\zeta} = \mathbb{R}^2_{>0}$, one can choose ϵ_1 with $0 < \epsilon_1 < \epsilon_0$ such that $\boldsymbol{x}(0) \in \bigcup_{\epsilon\in[\epsilon_1,\epsilon_0+\zeta]} \mathcal{M}_\epsilon$. We will prove that $\boldsymbol{x}(t) \in \mathcal{M}_{\epsilon_0}$ for a large enough t.

Towards this, let $\partial\mathcal{M}_\epsilon$ denote the boundary of $\mathcal{M}_\epsilon$. Define a function $\Upsilon : \bigcup_{\epsilon\in[\epsilon_1,\epsilon_0+\zeta]} \partial\mathcal{M}_\epsilon \to \left[\frac{1}{\epsilon_0+\zeta}, \frac{1}{\epsilon_1}\right]$ so that $\Upsilon(x,y) = \frac{1}{\epsilon}$ if $(x,y) \in \mathcal{M}_\epsilon$. We will show that $\Upsilon(\boldsymbol{x}(t)) \leq \frac{1}{\epsilon_0}$ for a large enough t. Let us assume that this is not true. By Lemma, we know that the sets $\Upsilon^{-1}\left(0, \frac{1}{\epsilon_0}\right] = \mathcal{M}_{\epsilon_0}$ and $\Upsilon^{-1}\left(0, \frac{1}{\epsilon_1}\right] = \mathcal{M}_{\epsilon_1}$ are invariant. This implies that $\Upsilon(\boldsymbol{x}(t)) \in [\frac{1}{\epsilon_0}, \frac{1}{\epsilon_1}]$ for all $t \geq 0$.

Note that the function Υ is differentiable everywhere except at the intersection points of the curves corresponding to the uncertainty regions, this corresponds to the points A, B, C, D. We will denote the curve that contains such points where Υ is not differentiable by $C_j(\epsilon)$. To proceed, we need to use some machinery from convex analysis. Towards this, for each curve C_j, let Υ_{j1} and Υ_{j2} be two functions such that $\Upsilon = \Upsilon_1$ on one side of C_j and $\Upsilon = \Upsilon_2$ on the other side. We now consider the following cases.

- *The angle made by $\mathcal{M}_\epsilon$ along C_j is $\leq \pi$*: We let $\Upsilon(\boldsymbol{x}) = \max(\Upsilon_{j1}(\boldsymbol{x}), \Upsilon_{j2}(\boldsymbol{x}))$ in a neighbourhood of the curve C_j. Defining $\Upsilon(\boldsymbol{x})$ this way ensures that $\Upsilon(\boldsymbol{x})$ is lower C^1 [20]. The subgradient of $\Upsilon(\boldsymbol{x})$ along $C_j(\epsilon)$ is given by

$$\partial\Upsilon(\boldsymbol{x}) = \{\gamma\nabla\Upsilon_{j1}(\boldsymbol{x}) + (1-\gamma)\Upsilon_{j2}(\boldsymbol{x}) \mid \gamma \in [0,1]\}. \tag{5.3.15}$$

Using the continuity of Υ, we can apply the chain rule of gradients [20, Theorem 10.6] to get

$$\partial(\Upsilon \circ \boldsymbol{x})(t) \subset \{\boldsymbol{z} \cdot \dot{\boldsymbol{x}}(t) \,|\, \boldsymbol{z} \in \partial\Upsilon(\boldsymbol{x}(t))\}. \tag{5.3.16}$$

Note that Lemma shows that $\mathcal{M}_\epsilon$ is invariant, i.e., the vector field along its boundary points towards $\mathcal{M}_\epsilon$. Consider a compact neighbourhood $\mathcal{K}$ of the curve C_j. Then we have $\dot{\boldsymbol{x}} \cdot \Delta\Upsilon_{j1} < 0$ and $\dot{\boldsymbol{x}} \cdot \Delta\Upsilon_{j2} < 0$ on $\mathcal{K}$. Now since $\mathcal{K}$ is compact, there is a $\delta > 0$ such that $\dot{\boldsymbol{x}} \cdot \Delta\Upsilon_{j1} < -\delta$ and $\dot{\boldsymbol{x}} \cdot \Delta\Upsilon_{j2} < -\delta$ on $\mathcal{K}$. From 5.3.15, we get that there exists a $\delta > 0$ such that $\boldsymbol{z} \cdot \dot{\boldsymbol{x}}(t) < -\delta < 0$ for all $\boldsymbol{z} \in \partial\Upsilon(\boldsymbol{x}(t))$ in $\mathcal{K}$. Using 4.4.4, we get

$$\sup_{t \geq 0} \partial(\Upsilon \circ \boldsymbol{x})(t) < -\delta. \tag{5.3.17}$$

Since Υ is lower C^1, one can apply the mean value theorem [20, Theorem 10.48] to $\Upsilon \circ \boldsymbol{x}(t)$ to get that there is a $\tau \in [0, t]$

$$\Upsilon(\boldsymbol{x}(t)) - \Upsilon(\boldsymbol{x}(0)) = t\alpha_t \text{ for some } \alpha_t \in \partial(\Upsilon \circ \boldsymbol{x})(\tau). \tag{5.3.18}$$

This implies that on $\mathcal{K}$, we have

$$\Upsilon(\boldsymbol{x}(t)) < \Upsilon(\boldsymbol{x}(0)) - \alpha t \tag{5.3.19}$$

for all $t > 0$. This contradicts the fact that $\Upsilon(\boldsymbol{x}(t)) \in [\frac{1}{\epsilon_0}, \frac{1}{\epsilon_1}]$ for all $t > 0$.

- *The angle made by $\mathcal{M}_\epsilon$ along C_j is $\leq \pi$*: We let $-\Upsilon(\boldsymbol{x}) = \max(-\Upsilon_{j1}(\boldsymbol{x}), -\Upsilon_{j2}(\boldsymbol{x}))$ in a neighbourhood of the curve C_j. Again, this ensures that $\Upsilon(\boldsymbol{x})$ is lower C^1.

□

Theorem 5.3.11. *Consider a dynamical system $\mathcal{G}_\epsilon^{\text{variable-k}}$. Then $\mathcal{M}_\epsilon$ is the minimal globally attracting region for $\mathcal{G}_\epsilon^{\text{variable-k}}$.*

Proof. This shows that M is a globally attracting region. We now show that it is minimal. Since the diagonal points are global attractors from the argument above, one can run the trajectories starting from these points to get the boundary of M. Therefore M must be contained in every globally attracting region, implying that M is a minimal globally attracting region. □

Theorem 5.3.12. *Consider a dynamical system $\mathcal{G}_\epsilon^{\text{variable-k}}$. Then, $\mathcal{M}_{\text{variable-k}}$ is the minimal invariant region for $\mathcal{G}_\epsilon^{\text{variable-k}}$.*

Proof. We now show that M is a minimal invariant region. Consider any invariant region A. We will show that $M \subseteq A$. For contradiction, assume that $\boldsymbol{x} \in M$ but $\boldsymbol{x} \notin A$. Now choose $B \in A$ and rate constants so that $\boldsymbol{x}$ is a global attractor for these values of rate constants. This can be done since M is a globally attracting region from above. This contradicts the fact that A is invariant. □

5.4 Minimal invariant region and minimal globally attracting region of two reaction with different directions

Now we discuss what happens in the case $5, 6$ where two reactions have their line generators in the different directions.

In cases $5, 6$, for ϵ small enough the region $\mathcal{M}_\epsilon$ can be constructed in the following

way.

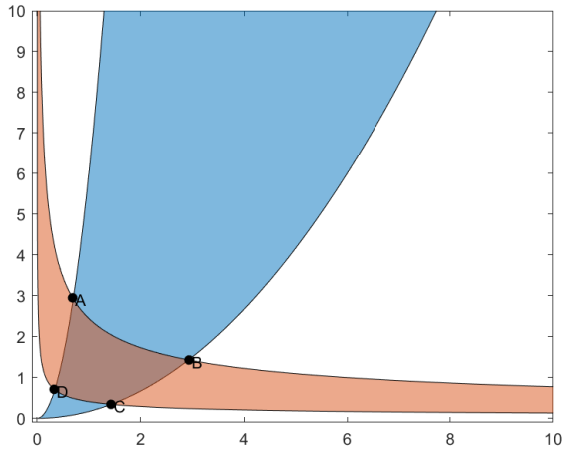

Figure 5.6: The uncertainty regions of case 5

Proof. We now prove the case 5, the case 6 can be proved with the same idea.

$$\begin{aligned} a_1X + b_1Y &\underset{k_2(t)}{\overset{k_1(t)}{\rightleftharpoons}} a_1'X + b_1'Y \\ a_2X + b_2Y &\underset{k_4(t)}{\overset{k_3(t)}{\rightleftharpoons}} a_2'X + b_2'Y \end{aligned} \tag{5.4.1}$$

Since $\frac{a_1-a_1'}{b_1'-b_1} > 1$ and $\frac{a_2-a_2'}{b_2'-b_2} < 0$.

Assume $p_1 = a_1 - a_1' > q_1 = b_1' - b_1 > 0$, $p_2 = a_2 - a_2' < 0$, $q_2 = b_2' - b_2 > 0$.

The boundary of the uncertainty regions:

$y^{q_i} = \epsilon^2 x^{p_i}$, or $y^{q_i} = \frac{1}{\epsilon^2} x^{p_i}$,

the point B and D:

$x_C = \epsilon^{2\frac{q_1-q_2}{p_1q_2-q_1p_2}}$, $x_D = \epsilon^{2\frac{q_1+q_2}{p_1q_2-q_1p_2}}$

For the lower red curve :

$$y'(x_C) = \frac{p_2}{q_2}\epsilon^{\frac{2(p_1-p_2-q_1+q_2)}{q_1(p_1q_2-q_1p_2)}} \tag{5.4.2}$$

Since $\frac{2(p_1-p_2-q_1+q_2)}{q_1(p_1q_2-q_1p_2)} > 0$, $y'(x_C) \to 0_-$ as $\epsilon \to 0$

$$y'(x_D) = \frac{p_2}{q_2}\epsilon^{\frac{2(p_1+p_2-q_1-q_2)}{q_1(p_1q_2-q_1p_2)}} \tag{5.4.3}$$

There are three subcases:

(a) $p_1 + p_2 - q_1 - q_2 < 0$, we can find a point E, the trajectories go from E to C, D will be part of the boundary of the minimal invariant region.

For the lower red curve, since $y'(x_D) \to -\infty$ and $y'(x_C) \to 0$ as $\epsilon \to 0_-$, so there is a point E which has the same slope as the blue attracting direction, and we can prove that from the point E, the trajectories to C and D will stay inside the blue uncertainty region $R(CD)$.

To prove that the trajectory $traj(ED)$ stay inside the region $R(CD)$, first notice that on the lower red curve $C_3(ED)$, the slope increase monotonically on the closed interval $[\frac{p_2}{q_2}\epsilon^{\frac{2(p_1+p_2-q_1-q_2)}{q_1(p_1q_2-q_1p_2)}}, -\frac{q_1}{p_1}]$, by applying the lemma 5.3.1 we get that the trajectory $traj(ED)$ can not cross the lower red curve $C_3(ED)$. Because the cone of the attracting direction in $R(CD)$ is contained in the first and second quadrants, so $traj(ED)$ won't go across

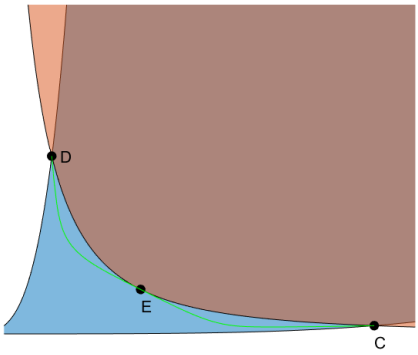

Figure 5.7: We start from a special point E and build trajectory $traj(EC)$ and $traj(ED)$.

the lower blue curve $C_1(OC)$ either.

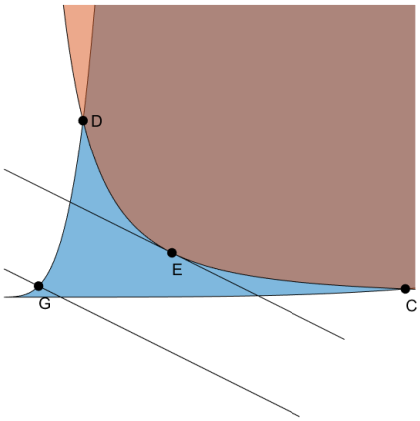

Figure 5.8: These two trajectories $traj(EC)$ and $traj(ED)$ will stay inside the region $R(CD)$

Now we want to show that the trajectory $traj(ED)$ won't go cross the upper blue curve $C_2(OD)$.

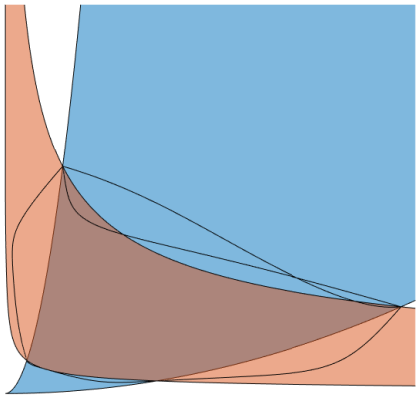

Figure 5.9: The closed region bounded by the curves $traj(AB)$, $traj(BA)$, $traj(BC)$, $traj(EC)$, $traj(ED)$ and $traj(AD)$ is the minimal invariant and the minimal globally attracting region

First we calculate the coordinate of E

$$\begin{aligned} f_3'(x) &= \frac{p_2}{q_2}\epsilon^{\frac{2}{q_2}}x^{\frac{p_2-q_2}{q_2}} \\ f_3'(x_E) &= -\frac{q_1}{p_1} \\ x_E &= (-\frac{q_1q_2}{p_1p_2})^{\frac{q_2}{p_2-q_2}}\epsilon^{-\frac{2}{p_2-q_2}} \\ y_E &= \epsilon^{\frac{2}{q_2}}x_E^{\frac{p_2}{q_2}} = (-\frac{q_1q_2}{p_1p_2})^{\frac{p_2}{p_2-q_2}}\epsilon^{-\frac{2}{p_2-q_2}} \end{aligned} \tag{5.4.4}$$

Denote the point F be the point on the upper blue curve C_1 where the tangent slope is equal to the red attracting direction.

$$
\begin{aligned}
f_2'(x) &= \frac{p_1}{q_1}\epsilon^{-\frac{2}{q_1}}x^{\frac{p_1-q_1}{q_1}} \\
f_2'(x_G) &= -\frac{q_2}{p_2} \\
x_G &= (-\frac{q_1q_2}{p_1p_2})^{\frac{q_1}{p_1-q_1}}\epsilon^{\frac{2}{p_1-q_1}} \\
y_G &= (-\frac{q_1q_2}{p_1p_2})^{\frac{p_1}{p_1-q_1}}\epsilon^{\frac{2}{p_1-q_1}-\frac{2}{p_1}+\frac{2}{q_1}}
\end{aligned}
\tag{5.4.5}
$$

Compare the exponent, since $p_1+p_2-q_1-q_2<0$ we have $-\frac{2}{p_2-q_2}<\frac{2}{p_1-q_1}<\frac{2}{p_1-q_1}-\frac{2}{p_1}+\frac{2}{q_1}$. To make sure that the point F can not be reached by the $traj(ED)$, we can check the level curve with the slope $-\frac{q_1}{p_1}$.

$$
\begin{aligned}
& y_G-(-\frac{q_1}{p_1})x_G-[y_E-(-\frac{q_1}{p_1})x_E] \\
&= \frac{1}{p_1}[p_1y_F+q_1x_F-p_1y_E-q_1x_E] \\
&\to -\frac{1}{p_1}(p_1y_E+q_1x_E) \quad \text{as } \epsilon\to 0
\end{aligned}
\tag{5.4.6}
$$

Note that $-\frac{1}{p_1}(p_1y_E+q_1x_E)<0$, therefore

$$
y_G+\frac{q_1}{p_1}x_G<y_E+\frac{q_1}{p_1}x_E \quad \text{as } \epsilon\to 0 \tag{5.4.7}
$$

, therefore if the trajectory $traj(ED)$ intersect with the curve $C(OG)$ at some point H(other than D), then H has a large y coordinate than the point G. The tangent slope $f_2'(x_H)>-\frac{q_2}{p_2}$, so at the point H, the attracting direction has the slope $-\frac{q_2}{p_2}$ less than the tangent slope of the curve, thus the attracting direction will point inside $R(CD)$. Therefore $traj(ED)$ will stay inside $R(CD)$.

So we can apply the lemma 5.3.1 to show that the trajectory $traj(ED)$ won't go across

the curve part $C_2(GD)$, since $traj(ED)$ won't go across any point whose y coordinate is small then y_F, therefore $traj(ED)$ would not go across the curve part $C_2(AG)$ either. Therefore $traj(ED)$ and $traj(EC)$ would stay inside the region $R(CD)$.

And we can prove that there are trajectories from A to D and from B to C which stay outside the uncertainty region. And for the upper red curve, since $y'(x_A) \to -\infty$ and $y'(x_B) \to 0$, there are two possible trajectories to form the outer bound of the region, we choose the one with larger value in y direction, and we can prove that in this way the curve will always stay outside the region $ABCD$.

(b) $p_1 + p_2 - q_1 - q_2 > 0$, this will lead to similar results as the subcase (a).

In this subcase, the slope $f_2'(x_D) \to 0$, $f_3'(x_D) \to 0$ and $f_1'(x_B) \to \infty$, $f_4'(x_B) \to \infty$ as $\epsilon \to 0$. this is analogous to the subcase (a), we can prove that with ϵ small enough the minimal invariant region $\mathcal{M}_\epsilon$ has boundaries formed by the trajectories $traj(AB)$, $traj(EB)$, $traj(EC)$, $traj(DC)$ and the union of $traj(DA)$ and $traj(AD)$.

(c) $p_1 + p_2 - q_1 - q_2 = 0$, this will be a combination of the previous situations.

In this case, the point B, D are on the line $y = x$, the slopes of the red curve and blue curve will not change with ϵ at the points B, D. And we have the following equality

$$\begin{aligned} f_1'(x_B) = f_2'(x_D) = \frac{p_1}{q_1} \\ f_3'(x_D) = f_4'(x_B) = \frac{p_2}{q_2} \end{aligned} \tag{5.4.8}$$

Let E be a point on the lower red curve CD which have the same tangent slope as the

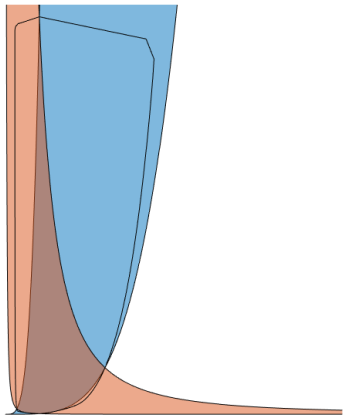

Figure 5.10: The minimal invariant region and the minimal globally attracting region for case 5(c)

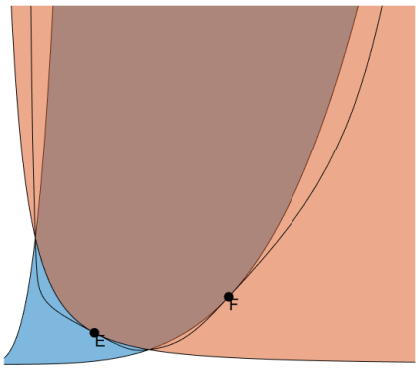

Figure 5.11: In this case the point E, F are inside the uncertainty regions and the point E',F' are outside the uncertainty regions.

blue attracting direction, and E' be a point on the upper red curve AB which have the same tangent slope as the blue attracting direction.

Assume the tangent on the lower red curve at the point C is k, then the tangent slopes are monotonically decreasing on CD in the range $[k, \frac{p_2}{q_2}]$, similarly, on the upper curve AB, they are monotonically decreasing in the range $[\frac{p_2}{q_2}, \frac{a}{k}]$ while a is a positive constant. Therefore, there is at most one point E or E' on the interior of the red curves AB or CD. When ϵ is small enough, we would get the minimal invariant region either like case a or the upper part AB is like case a while the lower part CD like subcase (b); or the upper part AB is like case b while the lower part CD like subcase (a). Similarly on the blue curves AD and BC we have one of the special point F or F' inside the red uncertainty region, and we can build the boundaries of the invariant region by following the same rules.

□

Theorem 5.4.1. *The regions $\mathcal{M}_\epsilon$ is the minimal invariant region for the variable-k dynamical system when ϵ is small enough.*

Proof. We are assuming $\epsilon > 0$ is small enough for all the discussion below.

For the case $5(a)$, when ϵ is small enough, the region $\mathcal{M}_\epsilon$ is constructed in the same way as the previous four cases. So we can prove it in a similar way.

For the case $5(b)$, on the upper red curve AB, the tangent slope changes continuously on the interval $[a, b]$ from the point A to the point B, and $a \to -\infty$, $b \to 0_-$ as $\epsilon \to 0$. and the blue attracting direction $-\frac{p_1}{q_1}$ is a fixed negative slope, so both trajectories from the point A to the point B and from the point B to the point A will enter the blue uncertainty

region above. Let's assume they intersect and the point M, then the trajectories AM and MB will form the outer bound of the minimal invariant region in this part. To prove this, first we want to prove that the point M is outside the closed region $ABCD$. The trajectory AB and BA are both outside the region at first, if we are entering the region $ABCD$, we need the slope k of the lower red curve to satisfy $k > -\frac{p_1}{q_1}$ for AB, and $k < -\frac{p_1}{q_1}$ for BA, this cannot be achieved at the same time, therefore, the intersection of the trajectories AB and BA cannot be inside the region $ABCD$. Therefore the curve AMB stay in the closed blue region and its tangent lines are bounded by some fixed proper cone, then we can apply the similar calculation in the previous section to show that the curve AMB is the outer bound.

On the lower red curve CD, we can find the point E inside the interval where the slope of the lower red curve equals $-\frac{q_1}{p_1}$ which is the slope of the blue attracting direction. We proved that the curve DEC stay inside the closed region $R(CD)$ and its attracting direction is bounded by a proper cone with slope $[-\frac{q_1}{p_1}, -\frac{q_2}{p_2}]$, similar to the previous cases, we have the $traj(ED)$ and $traj(EC)$ form the outer bound of the minimal invariant region in the region $R(CD)$.

In the case $5(c)$, the points E or E' are on the region $R(ABCD)$, the construction is a combination of $5(a)$ and $5(b)$. It can be proved analogously. □

Now we've already proved that the region $\mathcal{M}_\epsilon$ is the minimal invariant region for the variable-k dynamical system in cases $5, 6$, we can also show that this region $\mathcal{M}_\epsilon$ is also the minimal globally attracting region.

Theorem 5.4.2. *The regions $\mathcal{M}_\epsilon$ is the minimal globally attracting region for the variable-k dynamical system when ϵ is small enough.*

The proof of the theorem 5.4.2 is similar to the proof in theorem 5.3.11.

Now we have a method to construct the minimal invariant region and the minimal globally attracting region for any two reversible reactions in $2-D$. in the next section, we will discuss some results for the dynamical systems with more reactions in $2-D$.

5.5 Minimal invariant region and minimal globally attracting region of three reactions

With three reversible reactions, the systems may not be complex-balanced anymore, this will make it more difficult to specify the behavior of some special trajectories.

Now, we will give two examples and state our conjectures for three reaction cases.

Example 5.5.1.

$$\begin{aligned} Y &\underset{k_2}{\overset{k_1}{\rightleftharpoons}} 2X \\ 2X &\underset{k_4}{\overset{k_3}{\rightleftharpoons}} X+2Y \\ X+2Y &\underset{k_6}{\overset{k_5}{\rightleftharpoons}} Y \end{aligned} \tag{5.5.1}$$

This network is reversible and has deficiency 0. Therefore, according to the deficiency zero theorem, for all choice of rate constant $k_i \in (\epsilon, \frac{1}{\epsilon})$, the network is complex-balanced. Furthermore, the Horn-Jackson theorem applies, the mass-action system has a unique steady state within each stoichiometric compatibility class.

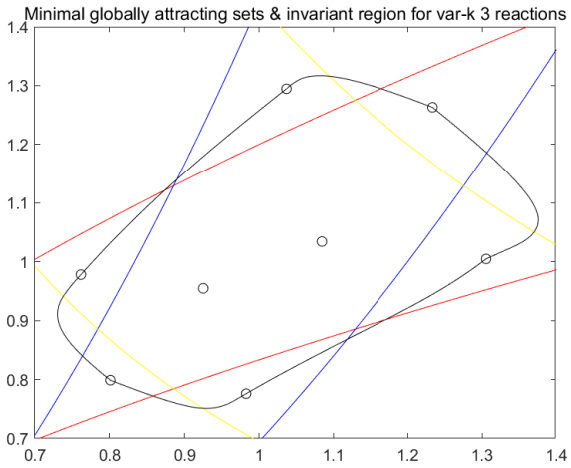

Figure 5.12: Three reactions example (complex-balanced)

Example 5.5.2.

$$\begin{aligned} 2X &\underset{k_2}{\overset{k_1}{\rightleftharpoons}} Y \\ X &\underset{k_4}{\overset{k_3}{\rightleftharpoons}} 2Y \\ X+Y &\underset{k_6}{\overset{k_5}{\rightleftharpoons}} \emptyset \end{aligned} \tag{5.5.2}$$

This network is reversible but the deficiency is not 0. We don't know whether the network is complex-balanced or not. But we have a conjecture that this minimal invariant region has the similar properties as the one in example 5.5.1.

In the three reactions mass action systems the network is not always complex-balanced. But we still have a conjecture that the minimal invariant region and the minimal globally attracting regions are the same, and in general they can be constructed by using some trajectories derived with some extreme choice of k values.

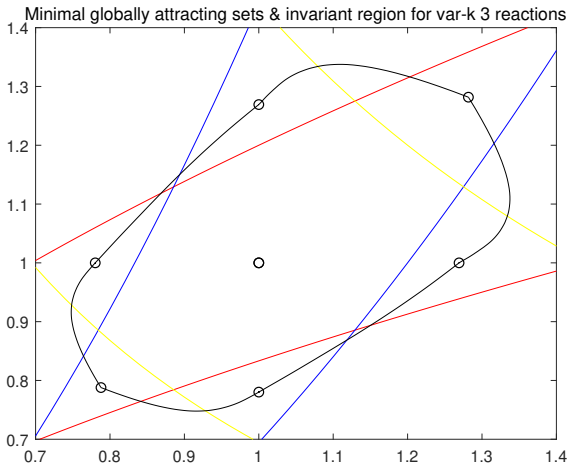

Figure 5.13: Three reactions example (not complex-balanced)

Appendix A

Some interesting results

Fixed-k dynamical system

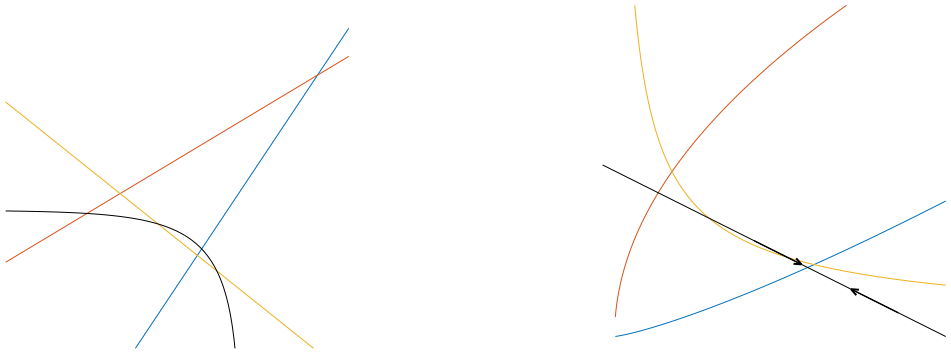

(a) Fixed-k dynamical system with three reactions(log)

(b) Fixed-k dynamical system with three reactions(exp)

Figure A.1

If we choose k in a proper combination, then we can show that the region marked in figure A.1(a) is not an invariant region.

With respect to figure A.1(b), we have the following observations

- Any fixed point must be inside this triangle.

- Any periodic orbit must intersect this triangle.

- If there is no periodic orbit or homoclinic/heteroclinic orbits, then the triangle is the globally attracting region.- By Poincare Bendixon.

We can prove that in some specific cases, there is a unique fixed point and therefore the periodic orbit won't exist. And we have the following conjectures:

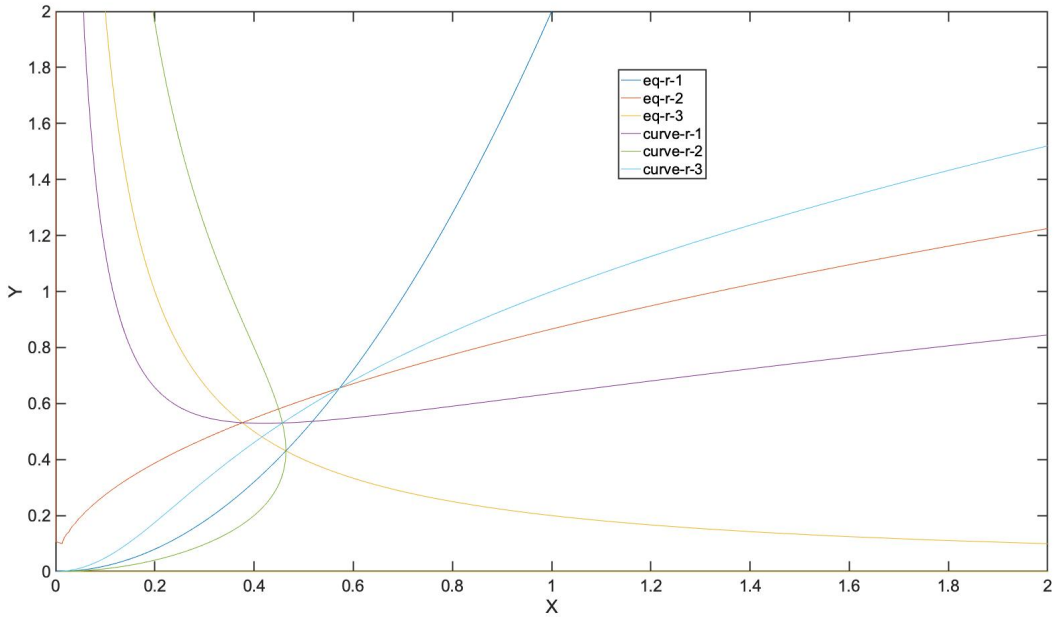

Figure A.2

Statements/Conjectures

- Three reversible reactions in two dimensions have a unique fixed point: This is not true. Counterexample: $\mathcal{G} = \{2A + B \rightleftharpoons 3A, A \rightleftharpoons \emptyset, B \rightleftharpoons \emptyset\}$. This does not have a unique fixed point.

- For three reversible reactions, if we construct some special curves where the attracting

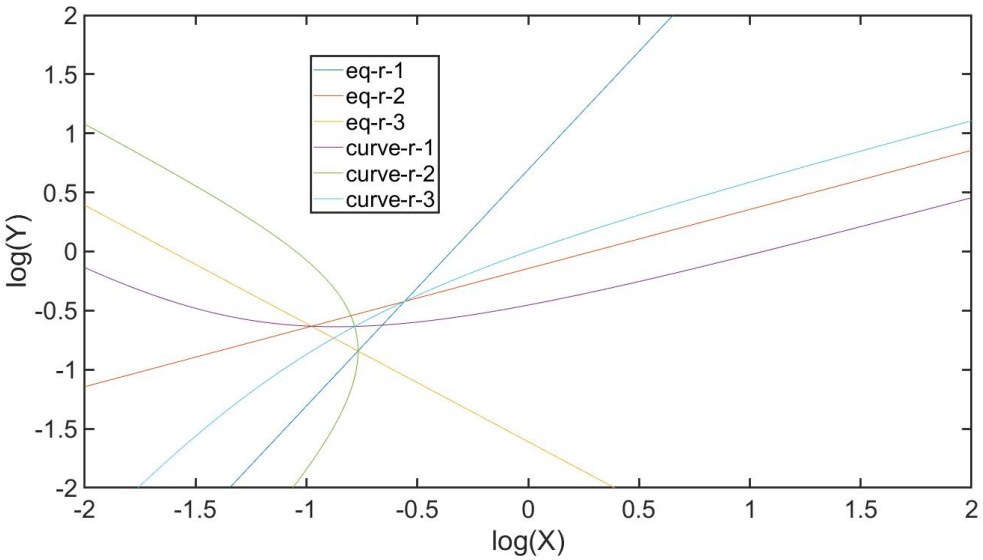

Figure A.3

direction vectors of the other two reactions will combine to get a new vector which have the same or opposite direction with the third vector, and if we can prove that two of the curves intersect only at one point inside the common 'triangular' region , then that point is the unique fixed point and there will be no periodic orbit.

- For any three reversible reactions, we might be able to show that there is no periodic orbit.

Bibliography

[1] D. F. Anderson, *A proof of the global attractor conjecture in the single linkage class case*, SIAM J. Appl. Math., 71 (2011), pp. 1487–1508.

[2] A. Berman and R. Plemmons, *Nonnegative matrices in the mathematical sciences*, SIAM, 1994.

[3] F. Blanchini, *Set invariance in control*, Automatica, 35 (1999), pp. 1747–1767.

[4] G. Craciun, *Toric differential inclusions and a proof of the global attractor conjecture*, arXiv preprint arXiv:1501.02860, (2015).

[5] G. Craciun, *Polynomial dynamical systems, reaction networks, and toric differential inclusions*, SIAM Journal on Applied Algebra and Geometry, 3 (2019), pp. 87–106.

[6] G. Craciun and A. Deshpande, *Endotactic networks and toric differential inclusions*, arXiv preprint arXiv:1906.08384, (2019).

[7] G. Craciun, A. Deshpande, and J. Yeon, *Quasi-toric differential inclusions*, arXiv preprint arXiv:1910.05426, (2019).

[8] G. Craciun, A. Dickenstein, A. Shiu, and B. Sturmfels, *Toric dynamical systems*, J. Symb. Comput., 44 (2009), pp. 1551–1565.

[9] G. Craciun, F. Nazarov, and C. Pantea, *Persistence and permanence of mass-action and power-law dynamical systems*, SIAM J. Appl. Math., 73 (2013), pp. 305–329.

[10] M. Feinberg, *Complex balancing in general kinetic systems*, Arch. Ration. Mech. An., 49 (1972), pp. 187–194.

[11] M. Feinberg, *Lectures on chemical reaction networks. notes of lectures given at the mathematics research center, university of wisconsin, madison, wi*, 1979.

[12] M. Feinberg and F. J. Horn, *Dynamics of open chemical systems and the algebraic structure of the underlying reaction network*, Chemical Engineering Science, 29 (1974), pp. 775–787.

[13] M. Gopalkrishnan, E. Miller, and A. Shiu, *A geometric approach to the global attractor conjecture*, SIAM J. Appl. Dyn. Syst., 13 (2014), pp. 758–797.

[14] C. Guldberg and P. Waage, *Studies concerning affinity*, CM Forhandlinger: Videnskabs-Selskabet i Christiana, 35 (1864), p. 1864.

[15] J. Gunawardena, *Chemical reaction network theory for in-silico biologists, 2003*, Bauer Center for Genomics Research, Harvard University, Cambridge, MA, 2138.

[16] F. Horn, *Necessary and sufficient conditions for complex balancing in chemical kinetics*, Archive for Rational Mechanics and Analysis, 49 (1972), pp. 172–186.

[17] F. Horn and R. Jackson, *General mass action kinetics*, Arch. Ration. Mech. An., 47 (1972), pp. 81–116.

[18] M. Nagumo, *Über die lage der integralkurven gewöhnlicher differentialgleichungen*, Proceedings of the Physico-Mathematical Society of Japan. 3rd Series, 24 (1942), pp. 551–559.

[19] C. Pantea, *On the persistence and global stability of mass-action systems*, SIAM J.

Math. Anal., 44 (2012), pp. 1636–1673.

[20] R. Rockafellar and R. Wets, *Variational analysis*, vol. 317, Springer Science & Business Media, 2009.

[21] P. Schuster, K. Sigmund, and R. Wolff, *On ω-limits for competition between three species*, SIAM Journal on Applied Mathematics, 37 (1979), pp. 49–54.

[22] Y. Takeuchi, *Global dynamical properties of Lotka-Volterra systems*, World Scientific, 1996.

[23] E. Voit, H. Martens, and S. Omholt, *150 years of the mass action law*, PLOS Comput. Biol., 11 (2015).

[24] P. Yu and G. Craciun, *Mathematical analysis of chemical reaction systems*, Isr. J. Chem., 58 (2018), pp. 733–741.